CONSIDERING THE OXYGEN EFFECT: FURTHER DEVELOPMENT OF A VOLUMETRIC MODEL OF TUMOR RESPONSE TO RADIATION THERAPY FOR CERVICAL CANCER

By

Stephanie S. Winkler

April 2014

Director of Thesis: Zhibin Huang, Ph.D.

Major Department: Physics

Mathematical modeling of tumor response to radiation therapy (RT) has great potential for designing therapy plans that are more personalized, more adaptive, and more reliable for outcome predictions. A preexisting model of tumor response to radiation therapy for cervical cancer has been shown to generate model parameters that correlate strongly with both tumor local control and disease-specific survival. This model is further developed through incorporation of another effect of RT not previously accounted for: the oxygen effect. An easily obtainable form of input data, hemoglobin level, enables simulation of the oxygen effect simultaneously with the other major model effects. For the Local Control (LC) patient group, the changes in the model parameters caused by incorporation of the oxygen effect are found to significantly improve the agreement of those parameters with actual patient data. For the Local Failure (LF) group and the overall patient group, the oxygen effect is incorporated without significant change to the agreement between the model-simulated output parameters and the actual patient data. Also, a strategy is presented for solving the main model equations to obtain analytic expressions for surviving cell fraction and regression volume ratio as functions of time.

CONSIDERING THE OXYGEN EFFECT: FURTHER DEVELOPMENT OF A VOLUMETRIC MODEL OF TUMOR RESPONSE TO RADIATION THERAPY FOR CERVICAL CANCER

A Thesis

Presented To

The Faculty of the Department of Physics

East Carolina University

In Partial Fulfillment of the Requirements for the Degree

Master of Science in Applied Physics

By

Stephanie S. Winkler

April 2014

CONSIDERING THE OXYGEN EFFECT: FURTHER DEVELOPMENT OF A
VOLUMETRIC MODEL OF TUMOR RESPONSE TO RADIATION THERAPY FOR
CERVICAL CANCER

By

Stephanie S. Winkler

APPROVED BY:

DISSERTATION ADVISOR_____
                                                            Zhibin Huang, Ph.D.

COMMITTEE MEMBER_____
                                                            Michael Dingfelder, Ph.D.

COMMITTEE MEMBER_____
                                                            Zi-Wei Lin, Ph.D.

COMMITTEE MEMBER_____
                                                            Orville Day, Ph.D.

CHAIR OF THE DEPARTMENT OF PHYSICS_____
                                                            Jefferson Shinpaugh, Ph.D.

DEAN OF THE GRADUATE SCHOOL_____
                                                            Paul J. Gemperline, Ph.D.

ACKNOWLEDGEMENTS

I would like to thank my advisor, Dr. Zhibin Huang, for giving me the opportunity to pursue research in kinetic modeling and for his constant guidance and mentorship over the course of this thesis. Dr. Huang has not only guided me through the technical aspects necessary to perform this research, but has also helped me become a more independent and creative researcher. I would also like to thank the Department of Physics for their support throughout my pursuit of this Master's degree. For providing extra guidance and important contributions to the quality of this work, special thanks are owed to the members of my committee: Dr. Zi-Wei Lin, Dr. Michael Dingfelder, and Dr. Orville Day. I would also like to thank Dr. Roberta Johnke for her indispensible advice on the interdisciplinary aspects of this work. Last but not least, I would like to thank my family for being a constant source of support and encouragement throughout this journey.

TABLE OF CONTENTS

LIST OF FIGURES AND TABLES

LIST OF ABBREVIATIONS

CBC   Complete Blood Count

DNA   Deoxyribonucleic Acid

DSB   Double-Strand Break

HGB   Hemoglobin

LC   Local Control

LDR   Low Dose Rate

LET   Linear Energy Transfer

LF   Local Failure

LQ   Linear Quadratic

MRI   Magnetic Resonance Imaging

OER   Oxygen Enhancement Ratio

RBC   Red Blood Cell

RT   Radiation Therapy

SRS   Simple Random Sample

SSB   Single-Strand Break

CHAPTER 1: INTRODUCTION

1.1 THE PROBLEM: Current RT plans are not adaptive, but more development is needed to make adaptive plans clinically feasible.

Only 30 to 40% of conventional radiation therapy (RT) treatments are successful at 2 years after treatment [1]. The definition of "success" here is a forgiving one, meaning simply that the patient is still alive. The success rate for cervical cancer treatments employing the conventional combination of RT and chemotherapy is higher, with a one-year success rate of 83.6% and a five-year success rate of 66.6% [2]. Even so, these statistics are unencouraging considering the sophisticated treatment modalities available, not to mention the wholehearted intellectual, emotional, and financial investments of patients, hospitals, and research organizations in the interest of managing this disease.

Despite extensive efforts to *customize* therapy, customized therapy plans are still not *adaptive* once they are in place. After a treatment plan is developed and approved, the plan is carried out over a period of 2 to 3 months with little reevaluation in the interim. However, radiobiological processes and hard-to-predict proliferative cancers can significantly change the state of a patient's illness in time frames much shorter than 2 months. By responding to these changes, adaptive therapy plans have the potential to improve treatment outcomes.

Though there are many reasons why cancer is difficult to manage, the issue of responding to a patient's changing status along the course of treatment is an issue that can be practically addressed using current knowledge and technology. Through use of physical, mathematical, and computational methods, adaptive therapy plans are feasible in a clinical setting. However, for adaptive therapy strategies to become the new standard-of-care, they must be not only feasible, but also be demonstrably worthwhile. The worthiness of such a strategy will depend on (a) how well it correlates with predictive power, and (b) the degree of confidence that can be assumed in

the strategy's predictions/conclusions. In 2006, Huang and colleagues developed a kinetic model of tumor regression during radiation therapy for cervical cancer. The model enables adaptive therapy by generating predictions about tumor survival that are personalized to each patient and based on time-dependent data. The model is based on three major effects of RT: radiation cell killing, tumor repopulation, and dead cell resolving. In 2010, the same group used long-term patient survival data to verify the model's predictive power in determining therapy outcomes, fully addressing (a). The next step is to refine the model in order to improve its accuracy, and hence improve (b), the degree of confidence clinicians can assume in its conclusions.

1.2 The Challenge: Improve the accuracy and scope of the preexisting adaptive therapy model by incorporating another major effect of RT.

As previously stated, the preexisting model is based on three major effects of RT: radiation cell killing, tumor repopulation, and dead cell resolving. However, the effects of RT are numerous. There are many possibilities for how to go about refining the model, but there are constraints on the potential refinements. First, it is critical that changes to the model are based on tenets of medical physics, radiobiology, or oncology. This way, the equations of the model remain scientifically meaningful. When developing quantitative descriptors of traditionally qualitative topics, it is more valuable to have a rough but meaningful mathematical description than a perfect but nonsensical description. The second constraint involves the type of input data from patients that the model may rely upon. Selection and use of input data must be respectful of the practical limitations on collecting patient data in the clinic. Ideally, input data should not impose additional pain or cost on the patient or require much additional labor from clinicians, beyond what is involved in conventional therapy. In accordance with this ideal, the preexisting model relies on easily obtainable MRI images and dose schedules as input data.

1.3 BACKGROUND INFORMATION

1.3.1   Cancer Biology: Hypoxia and Reoxygenation

Tumor biology is significantly different from normal tissue biology. Converse to normal tissues that possess a neat and efficient system of blood vessels, tumors exhibit "vascular chaos" resulting from their fast and erratic formation as the tumor grows quickly. This accelerated vessel growth is a result of angiogenic switch—the loss of balance between stimulation and inhibition hormones that control new blood vessel growth—and is a common characteristic of cancerous tumors [3]. Even so, new blood vessels often cannot be formed rapidly enough to meet the circulatory demands of the rapidly growing tumor. Consequently, existing vessels become elongated, twisted, and dilated in an effort to survive by increasing the area of the vessel walls, which function as a metabolic exchange area for nutrients, oxygen, hormones, and waste [4].

These twisted and dilated vessel networks do not function efficiently. Huang et. al. succinctly note, "Blood flow is generally erratic, sluggish, and intermittent, characterized by arteriovenous shunting [bypass], stasis [flow decline], and also reversal of blood flow within tumor vessels" [3]. As tumors continue growing and their vasculature becomes increasingly tortuous, circulatory disruptions like shunting, stasis, and reversal becomes increasingly consequential, resulting in tumor regions with poor or no circulation.

The key result of tumor vasculature irregularities and circulatory disruptions is that some parts of the tumor do not receive enough oxygen to support normal cell growth and functioning; this condition is called "hypoxia." A key feature of hypoxic cells is that they show radioresistance, meaning they are less susceptible to radiation-induced death [5]. There are two types of hypoxia: chronic and acute. Chronic hypoxia occurs because oxygen has a limited

diffusion distance in respiring tissue and does not always reach cells that are far from blood vessels. Acute hypoxia occurs due to random opening and closing of vascular pathways. Both chronic hypoxia and acute hypoxia are intermittent and regional. Prominent radiobiologist Eric Hall notes that tumor cells are "exposed to a continuum of oxygen concentrations" due to both forms of hypoxia [6]. As a result, both the fraction of hypoxic cells and their location will change in time. In a study of forty-two tumor types by Moulder and Rockwell, hypoxic fractions ranged from 0 to 50%, with an average result of about 15% [7].

The fact that hypoxia is intermittent and regional implies that tumors can become reoxygenated after having been hypoxic. The timescale of reoxygenation is particularly important in radiation therapy. In a series of experiments by van Putten, and Kallman on a variety of tumor systems, the *proportion* of hypoxic cells post irradiation returned to its pretreatment level within twenty-four hours [8]. It is widely believed that the mechanism of reoxygenation is as follows: radiation dose kills aerated cells, and once they are removed, formerly hypoxic cells can once again access diffuse oxygen to become reoxygenated, as shown in Figure 1. On this theory, Hall notes "Reoxygenation cannot be measured in human tumors, but presumably it occurs, at least in those tumors controlled by conventional fractionated radiotherapy" [6].
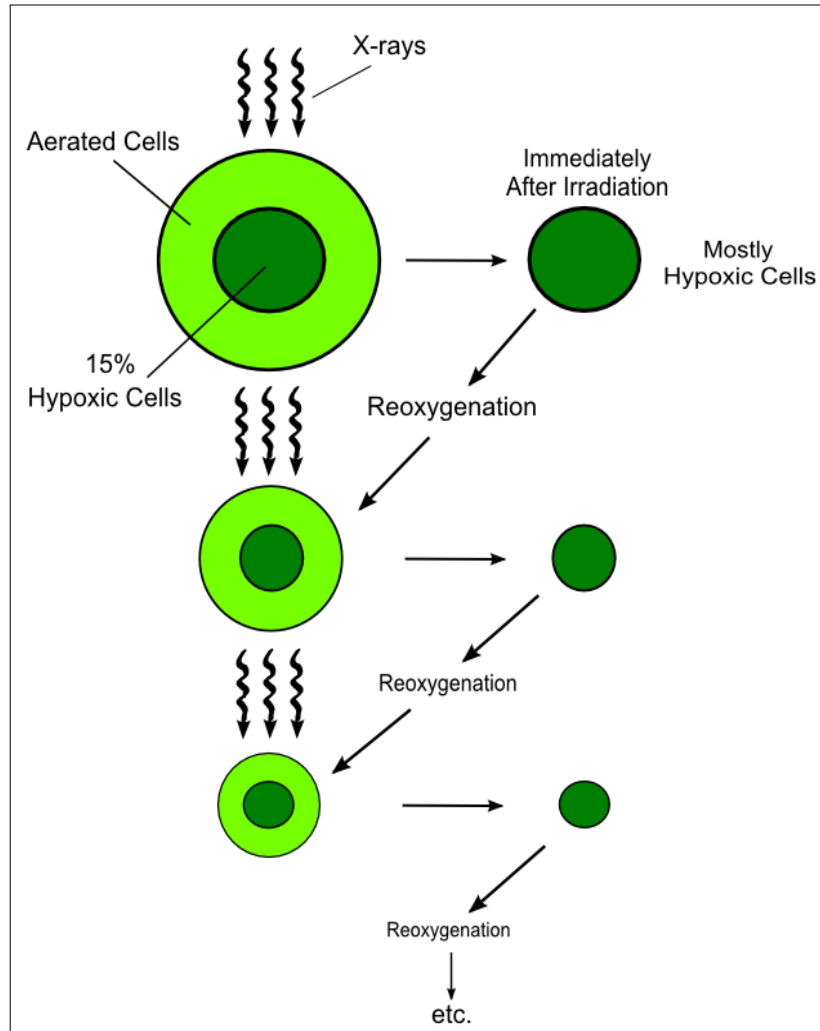
Figure 1. Tumor Reoxygenation

1.3.2 Radiation Biology and the Oxygen Effect

It has been mentioned above that lack of oxygen leads cells to become radioresistant. The corollary is also true; the presence of oxygen makes cells more radiosensitive. This is what is known as the "oxygen effect" [6]. The complexities of the oxygen effect will influence how it should (and reasonably can) be incorporated into an existing patient model.

The oxygen effect acts through two distinct mechanisms. Diatomic oxygen gas present in irradiated tissue (a) increases free radical production, and (b) "fixes" (i.e., makes permanent) the damage those free radicals cause. An estimated two thirds of the damage that x-rays produce in

biological tissue is due to indirect action on the part of free radicals, while the remaining one third results from direct "hits" made by the x-ray photons in the tissue [6].

The creation of free radicals occurs when radiation interacts with matter, causing larger molecules to be broken up by the sudden influx of energy. This creates atoms, molecules, or ions with unpaired valence electrons—otherwise known as free radicals [9]. The exact mechanisms by which this happens cannot be pinpointed, especially since it varies from tissue to tissue. However, the free radicals can be attributed to ionizing radiation interactions with water and with organic molecules specific to the tissue [10], which will be designated as "T" in this discussion.

The interaction of radiation with water forms the water radicals $\dot{O}H$ and $\dot{H}$ [10] as shown in Equations (1) and (2):

$$HOH \rightarrow e^- + (H\dot{O}H)^+ + \dot{O}H \tag{1}$$

$$HOH + e^- \rightarrow (HOH)^- \rightarrow \dot{H} + OH^- \tag{2}$$
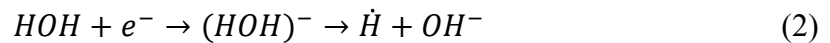
The water radicals have a strong affinity for electrons, and they remove Hydrogen atoms from other molecules, "R," that they encounter in the tissue [10] as shown in Equation (3):

$$\dot{O}H + RH \rightarrow \dot{R} + HOH \tag{3}$$

The water radicals will recombine to form water if they encounter one another before interacting with tissue [10].

The interaction of radiation with tissue is presented by radiation biologist M. Quintiliani in terms of the tissue-specific organic molecule T [11] in Equation (4):

$$TH + \gamma \rightarrow \dot{T} + O_2 \rightarrow T\dot{O}_2 \tag{4}$$

The processes shown in Equations (1) through (4) occur with or without diatomic oxygen being present in the irradiated tissue. However, the presence of oxygen increases the number and type of free radicals produced and thus increases biological damage.

In addition to producing more of the water and tissue radicals described above, the presence of oxygen results in an additional type of radical—monatomic oxygen radicals. Diatomic oxygen molecules that are hit directly by ionizing radiation produce monatomic oxygen radicals [12] as shown in Equation (5):

$$O_2 \rightarrow \dot{O} + \dot{O} \tag{5}$$

As various radicals interact with biological matter and with one another, significant biochemical changes occur. Chemical bonds are broken, and new ones are formed, and DNA strand breaks occur that alter cells' reproductive blueprints. The cumulative result of this chemical damage is expressed as future biological damage [10].

In addition to increasing free radical production, oxygen present during irradiation also disables repair mechanisms that can counteract free radical damage, thus making that damage permanent by initiating a permanent chemical change. Significantly, in the absence of oxygen, the radical $\dot{T}$ can be repaired by hydrogen donation from a sulfhydryl compound or other hydrogen-donating molecules [11]. However, once the tissue-specific radical $\dot{T}$ reacts with O_2, it forms an organic peroxide in a one-way chemical reaction [10] as shown in Equation (6):

$$\dot{T} + O_2 \rightarrow T\dot{O}_2 \tag{6}$$
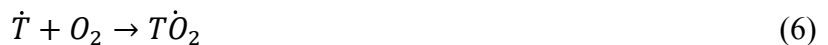
The organic peroxide cannot be changed back to the original organic material, so the damage is made permanent on the molecular level, thus "fixing" the damage in place.

Quintiliani discusses the difficulty of identifying the precise structure of the tissue-specific molecules T involved in the oxygen effect. Throughout the literature it is agreed upon that the oxygen effect acts mainly on the critical target of DNA [6, 13, 14] a molecule for which mapping molecular structure is notorious complicated. Though exact mechanisms cannot be identified, Chapman estimates that 82% of radiation-induced cell death for aerated cells is caused

by the fixation of free radical damage—refer to Equations (1) through (3), and (5) through (6)—while the remaining 18% is caused by direct action of x-ray photons with tissue—Equation (4) [10].

The overall impact of the oxygen effect is quantified in terms of the Oxygen Enhancement Ratio (OER). The OER is the ratio of doses required under hypoxic conditions vs. aerated conditions to achieve the same biological effect. For x-rays, the OER is between 2.5 and 3.5, increasing with dose [6]. The dramatic impact of oxygen as a radiosensitizer is due in part to the very small time window required to initiate the oxygen effect and to the low gas tensions (pressures) at which effects begin to be seen. For the oxygen effect to be observed, oxygen needs to be present during or within microseconds of irradiation. This is because the chemical reactions that produce the free radicals and "fix" damage have lifetimes on the order of 10 microseconds at the longest [6]. In the living body of a patient, the condition for oxygen presence during or within microseconds of irradiation is easily met, except in hypoxic regions. Very low concentrations of oxygen are sufficient to sensitize mammalian cells to radiation, with full saturation of the oxygen effect occurring around 30 mm Hg, and significant sensitization occurring as low as 3 mm Hg. For comparison, normal venous tissue has an oxygen tension of 20 – 40 mm Hg [6].

The oxygen effect in RT has long been seen as a double-edged sword. A conundrum arises because the lack of oxygen prevents the tumor from growing and metastasizing, but it also makes the tumor resistant to conventional RT. Modern RT methods employ the duality of the oxygen effect to control tumor growth without compromising radiosensitivity.

1.3.3 Fractionated Radiotherapy and the Four R's

The body of knowledge on cancer biology and radiation biology has resulted in an almost universally accepted method of treating cancerous tumors in patients: fractionated radiotherapy. Relying on the concept of tumor reoxygenation, radiation doses delivered in strategic fractions can overcome tumor hypoxia while mitigating tumor growth.

A conventional fraction size is 1.8 – 2.0 Gy [3]. Typically, a patient receives one fractionated dosage per day for five days a week over a period of several weeks. The premise of this treatment is based on "the Four R's of Radiotherapy." They are *Repair, Reassortment, Repopulation*, and *Reoxygenation* [15]. *Repair* of sublethal damage takes place in normal tissue that has been exposed to radiation. Using a fractionated therapy schedule allows time for normal sublethal repair mechanisms to act. *Reassortment* of cells within the cell cycle as a response to irradiation can be used advantageously, since cells are more or less radiosensitive depending on what phase of the cell cycle they are in. For low doses like those used in fractionated RT, cells in the M phase, late G1 phase, and early S phase are the most radiosensitive [10]. By administering radiation doses regularly, clinicians can increase the chance of catching cells in a sensitive phase, hence increasing cell killing. *Repopulation* of normal cells is a controlled process, but for tumors, repopulation accelerates as tumor volume decreases, so frequent doses, or fractions, are needed to control tumor cell repopulation. *Reoxygenation*, as discussed above, allows hypoxic areas to become oxygenated again after the aerated cells that block them from diffuse oxygen are killed in RT and removed by the tumor's vasculature. Tumors are said to be fully reoxygenated when the original proportion of aerated cells is restored to its pre-irradiation value. Once reoxygenated, formerly hypoxic tumor cells are again subject to radiation induced death [15].

1.3.4   Quantifying Cell Survival

Any in-vivo model for tumor survival like the one presented in this thesis is based on the premise that cell survival can be quantified. Below is a discussion of early methods for quantifying cell survival, popular models of in-vitro cell survival, and the applicative power of cell survival models.

In 1956, Puck and Marcus developed the first cell survival curve, plotting the surviving fraction of irradiated cells as a function of dose [16]. "Survival" is defined in a cell assay as reproductive viability, so cells that are able to undergo division and produce a colony within an allotted time are said to have survived, while those that did not reproduce are considered dead [10]. Cell culture techniques allow the experimenter to control the number of cells being treated, so it is possible to predict how many individual colonies to expect [10]. By counting the number of colonies that form from a know number of individual cells, a rough estimate of the surviving fraction can be obtained. The conventional formula for cell survival in an assay is given by Equation (7):

$$S = \frac{\text{Number of Colonies Formed}}{\text{Number of Single Cells Plated} \; x \; (PE)_c} \tag{7}$$

where $(PE)_c$ is the plating efficiency of those cells, or the fraction of living cells that thrived into colonies after plating in a Petri dish or a flask [10]. Plating efficiency simply described the viable fraction of what was plated; there is no treatment (radiation) involved. A linear-linear plot of survival vs. dose produces an exponential curve or a sigmoidal curve, but the convention is to use a log-linear plot, which produces a "shoulder" at low doses, followed by a declining linear region, as can be seen in Figure 2a.
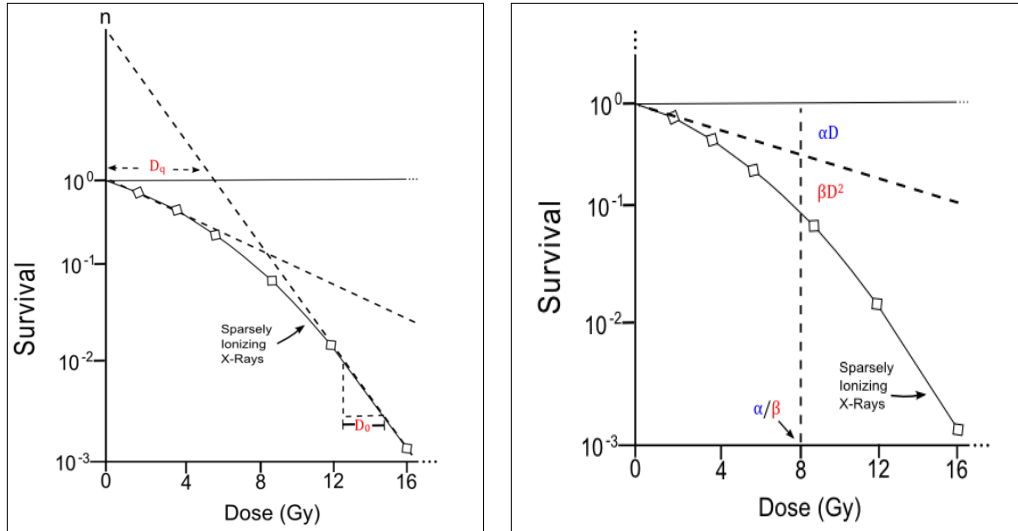
Figure 2. A characteristic shape for a cell survival curve is shown. At left, the curve is delineated with LQ model parameters D_q, D_0, and n. At right, it is delineated with LQ model parameters α and β.

Since the work of early radiobiologists Puck and Marcus, there have been several popular theories to account for the shape of survival curves and the mechanisms that produce them. Identifying critical targets in the cell, whose interaction with radiation produces death has been an important and controversial aspect of these theories. Early thoughts on the topic resulted in Hit Theory. This involved the idea that one radiation "hit" to a cell would cause death. Some postulated that there was a single critical target, while others assumed multiple critical targets, a hit to any one of which could cause cell death. Next, came Target Theory. This model posed the idea that cell death (or reproductive inability) was caused by the cumulative damage to several nonlethal targets. The cell membrane, DNA, proteins, and enzymes were all considered among the potential nonlethal targets [5].

Meanwhile, a large body of research was accumulating that strongly suggested DNA was the critical target for reproductive cell death [10]. The study of radiation induced single-strand breaks (SSB) and double-strand breaks (DSB) in the DNA's helical phosphate backbone lead to the linear-quadratic (LQ) model. It is based on the high likelihood of single-strand breaks at low

12

doses and the increasing predomination of double-strand breaks at higher doses. The LQ model attributes the linear "shoulder" of the survival curve to SSB, and the quadratic tail to DSB. Though newer models have been developed, the LQ model is still the standard in the laboratory and the clinic for its descriptive power and ease of use.

Cell survival curves are described in terms of the LQ model using several key parameters: D_0, D_q, and n, all of which are shown in Figure 2a. D_0 describes the slope of the linear region. Specifically, D_0 is the dose required to produce an average of one hit per target, thereby inactivating 63% (or 1-1/e) of the cells. D_q is the dose at which the exponential portion of the curve intercepts 100% survival when extrapolated back to the y-axis [10]. Closely related to D_q is the extrapolation number n, which is obtained by extrapolating the linear portion of the curve back to a dose of zero, and subtracting from it the initial surviving fraction of 1. Both n and D_q give an idea of the width of the shoulder region. The three parameters are related [10] by Equation (8):

$$D_q = D_0 \ln(n) \tag{8}$$

Perhaps even more clinically relevant than D_0, D_q, and n, are the parameters α and β. α describes the portion of cell kill caused by the linear component (SSB). β describes the portion of cell kill caused by the quadratic component (DSB) [10]. As seen in Figure 2b, the α/β ratio is the dose at which the two components contribute equally. Visually, this gives an idea of the width of the shoulder on the survival curve, and is very useful for determining early and late responses of cells to radiation. α and β are the key parameters [10] used in the survival equation for the LQ model, Equation (9):

$$S = e^{-(\alpha D + \beta D^2)} \tag{9}$$

Familiarity with the linear-quadratic model combined with known values of D_q, D_0, n, or just α/β enables clinicians to visualize the key features of any particular survival curve, including how the cells respond differently at low and high doses, and how that particular cell group may be compared with others. It is this ability to quickly glean rough information from a few simple numbers that makes this type of model so powerful and useful.

1.4 OVERVIEW OF THE ORIGINAL MODEL

Before addressing modifications made to the preexisting model, it is necessary to briefly describe that model. Again, the original model incorporates three major effects of RT: radiation cell killing, tumor repopulation, and dead cell resolving. Equations (10) are the "main model equations" as given by the developers, Huang and colleagues, in their 2010 publication [17]:

$$
\begin{cases}
\frac{dR(t)}{dt} = -\frac{\ln 2}{T_{1/2}}[R(t) - S(t)], \\
\frac{dS(t)}{dt} = S(t)\left[-(1 - S_2) + \frac{\ln 2}{T_d}\right]
\end{cases} \tag{10}
$$

where the time-dependent functions R(t) and S(t) are a tumor's regression volume ratio and surviving cell fraction, respectively. The other variables represent basic radiobiological parameters that correspond to the major effects of RT on which the model is based. $T_{1/2}$ is the half-time of dead cell resolving, obviously corresponding to the major effect of dead cell resolving. It is a gauge of how long it takes the tumor's vasculature to clear away cells that are reproductively dead. S_2 is the surviving cell fraction after a dose of 2 Gy, a measure of radiosensitivity corresponding to the major effect of radiation cell-killing. S_2 is a standard reference point in radiation oncology. T_d is the effective tumor doubling time, corresponding to the major effect of tumor repopulation. Whereas $T_{1/2}$ and S_2 are free parameters, T_d is held constant at a value of 3.5 days, an average taken from the literature [18-23].

The original model is based on a few major assumptions. It is assumed that when tumor cells are killed/inactivated by RT, the damaged cells lose their ability to reproduce, and eventually die. Then they are cleared from the area by blood circulation, by uptake of reticuloendothelial cells that process waste, or by surface sloughing. Clearing dead cells takes time, so immediate change in tumor volume after each RT fraction is not expected. It is assumed that the dead cell resolving proceeds in an exponential fashion. As more and more tumor cells

are killed and cleared, formerly hypoxic regions regain access to oxygen and nutrients, becoming reoxygenated. Then repopulation of surviving tumor cells begins [17].

It is useful to obtain regression volume ratio R(t) and surviving cell fraction S(t) for adaptive therapy purposes. However, solving Equations (10) requires knowledge of S_2, $T_{1/2}$, and T_d. For cervical cancer, T_d is taken as 3.5 days, as previously stated. In order to determine an individual patient's S_2 and $T_{1/2}$, a numerical calculation method is used to "fit" Equation (11) for volume as a function of day to a control curve generated from the patient's own MRI-volume and time data:

$$V_i = V_{s,i} + V_{d,i} \tag{11}$$

where V_i is the total tumor volume, $V_{s,i}$ is the portion of the volume composed of surviving cells (or living clonogens), and $V_{d,i}$ is the volume composed of dead cells that haven't been removed yet [17]. The determination of S_2 and $T_{1/2}$ comes in when you consider Equations (12) and Equation (13), the model's remaining "volume equations" for $V_{s,i}$ and $V_{d,i}$:

$$V_{s,i} = \begin{cases} V_{s,i-1}S_2^{n_i}, & \text{when } i \leq T_k, \\ V_{s,i-1}S_2^{n_i}e^{\ln(2)/T_d}, & \text{when } i > T_k, \end{cases} \tag{12}$$

$$V_{d,i} = V_{d,i-1}e^{-\ln2/T_{1/2}} + (V_{s,i-1} - V_{s,i}) \tag{13}$$

where n_i equals 1 for RT days and 0 for non-RT days [17]. T_k is the onset time of tumor repopulation, taken from the literature to be 21 days [24]. Equations (12) and (13) are based on a study by Bentzen and colleagues that demonstrated proportionality between clonogen number and tumor volume [17]. To summarize and restate, the volume equations—Equations (11) through (13)—are used to determine an individual patient's S_2 and $T_{1/2}$ through comparison with actual MRI volume and time data, as shown in Figure 3 below.
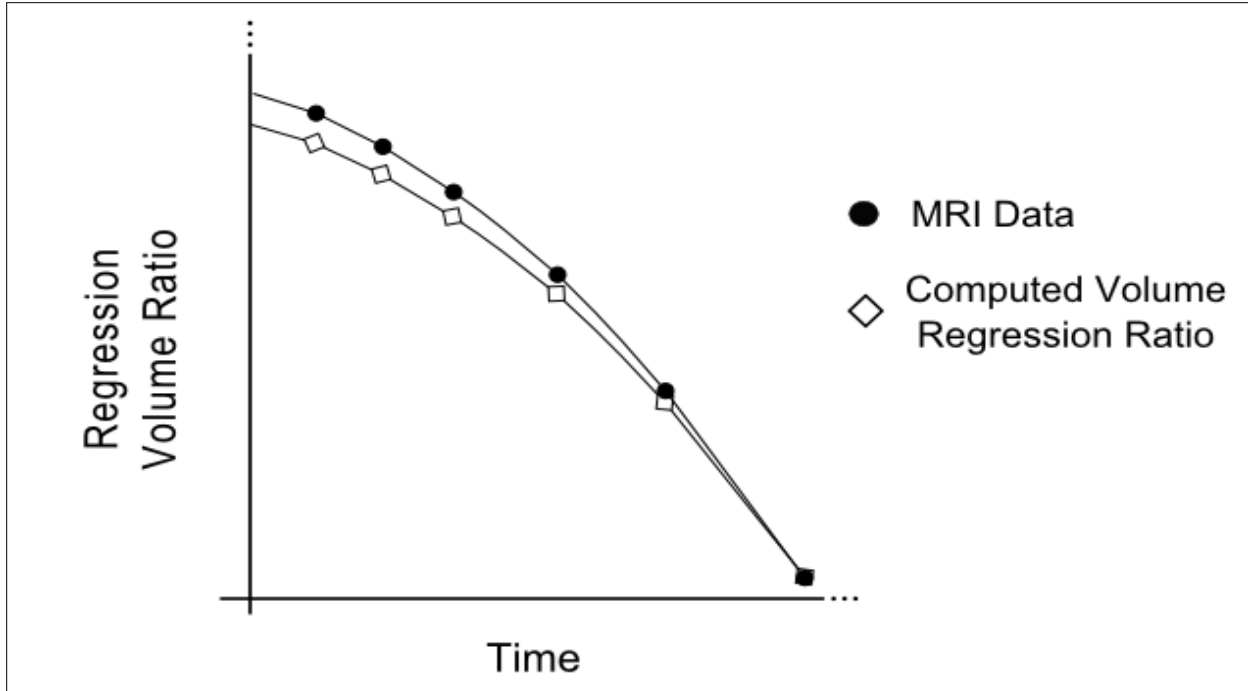
Figure 3. Varying S_2 and $T_{1/2}$ to produce computed data points, which are connected to form a curve. The computed curve is compared to the MRI data curve, and quantified using the "goodness of fit" X^2 statistic. The values of S_2 and $T_{1/2}$ that produce the best fitting curve are selected as output parameters for the individual patient. (Data shown here is hypothetical and is used for illustration purposes only.)

Although the goal is to ultimately obtain R(t) and S(t), Equations (11) through (13) use subscripts i—not continuous variable t—where i represents number of days into treatment. Because the main model equations describe *major* effects of RT (cell killing, tumor repopulation, and dead cell resolving) that produce detectable changes in volume over a timescale of days, time cannot be viewed as truly continuous within the framework of the volume equations, Equations (11) through (13). Using the subscripts i, the step size of time is given in days. Further discussion of step size limitations for time t is provided in Methods section 2.5.1.

The volume equations can be linked to the main model equations [17], Equations (10), by equating R_i with R(t) as shown in Equation (14):

$$R_i \cong R(t) \tag{14}$$

In the limit of increasing number of data points, i.e., taking MRI images more frequently, the sum over the increment i approaches a continuous function, like R(t). Another basis for equating R_i with R(t) is the similarity of their definitions; both R_i and R(t) represent a percentage of tumor volume at a given time normalized to the initial tumor volume [17], as in Equation (15):

$$\begin{cases} R_i = \frac{V_i}{V_0} \\ R(t) = \frac{V(t)}{V(0)} \end{cases} \tag{15}$$

Throughout this thesis, Equations (10) will be referred to as the "main model equations," and Equations (11) through (13) will be referred to as the "volume equations." The volume equations are used to determine patient-specific values for S_2 and $T_{1/2}$ computationally. The main model equations, using those patient-specific values of S_2 and $T_{1/2}$ from the volume equations, are solvable for R(t) and S(t).

1.5 DUAL OUTCOME: Clinical Parameters and Analytic Solution

It is important to note the dual application of the model.

Clinical Outcome

The output parameters S_2 and $T_{1/2}$ are useful estimates for describing tumor survival. In clinical settings, these parameters can give clinicians a rough idea of a tumor's survival curve very quickly and without any additional calculation. As an example, consider the common knowledge that a person's height and weight are a rough-but-good indication of their body type. A body mass index analysis is more technically correct, but is time consuming and difficult by comparison. A patient's S_2 and $T_{1/2}$ are much like their height and weight—not a complete description, but a useful easily obtained picture. Using a more technical example, S_2 and $T_{1/2}$ can also be compared to the LQ model's α and β because they also give an idea of the width of the shoulder and the rate of the decline in the linear region of the curve.

Mathematical Outcome

The output parameters S_2 and $T_{1/2}$ can be substituted into the main model equations as constants, enabling an analytic solution to be obtained for regression volume ratio R(t) and surviving cell fraction S(t). These expressions are the most complete description that can be obtained from the model. In R(t) and S(t) lies the obvious predictive power of the model, and the freedom to choose any t.

1.6 HYPOTHESIS AND SPECIFIC AIMS

It is the hypothesis of this thesis that incorporating a fourth major effect of RT into the model will improve the accuracy of its output parameters, increasing the degree of confidence that may be invested in those parameters. Specifically, the fourth effect to be incorporated is the oxygen effect. Since oxygen is abundant in living bodies, it is hypothesized that considering the oxygen effect will improve this in-vivo model of tumor survival as a response to RT by producing output values S_2 and $T_{1/2}$ that more closely correlate with clinical outcome data.

The specific aims of this research that enable testing of the hypothesis are as follows:

I.   Propose and test meaningful ways to modify the preexisting model to account for the oxygen effect by using average hemoglobin levels as the new input parameter. Develop C++ code(s) to tests these modifications. Ultimately, use that code to fit the parameters S_2 and $T_{1/2}$ for the each patient in the study using Equations (11) through (13).

II.   Use statistical analysis techniques to determine whether incorporating the oxygen effect into the model by adding in the hemoglobin level significantly changes the output parameters X^2 ("goodness of fit"), S_2, and $T_{1/2.}$

III.   Demonstrate the mathematical capabilities of the model by obtaining R(t) and S(t) analytically. Investigate the applicability of these expressions.

Successful completion of these specific aims can provide insight on in vivo modeling for RT. In the broader context, these are steps toward the goal of developing preliminary qualitative descriptions of phenomena that have traditionally been understood only qualitatively. Figure 3 below is a conceptual map of this thesis, illustrating how the patient data will be used to obtain a clinical outcome and a mathematical outcome.
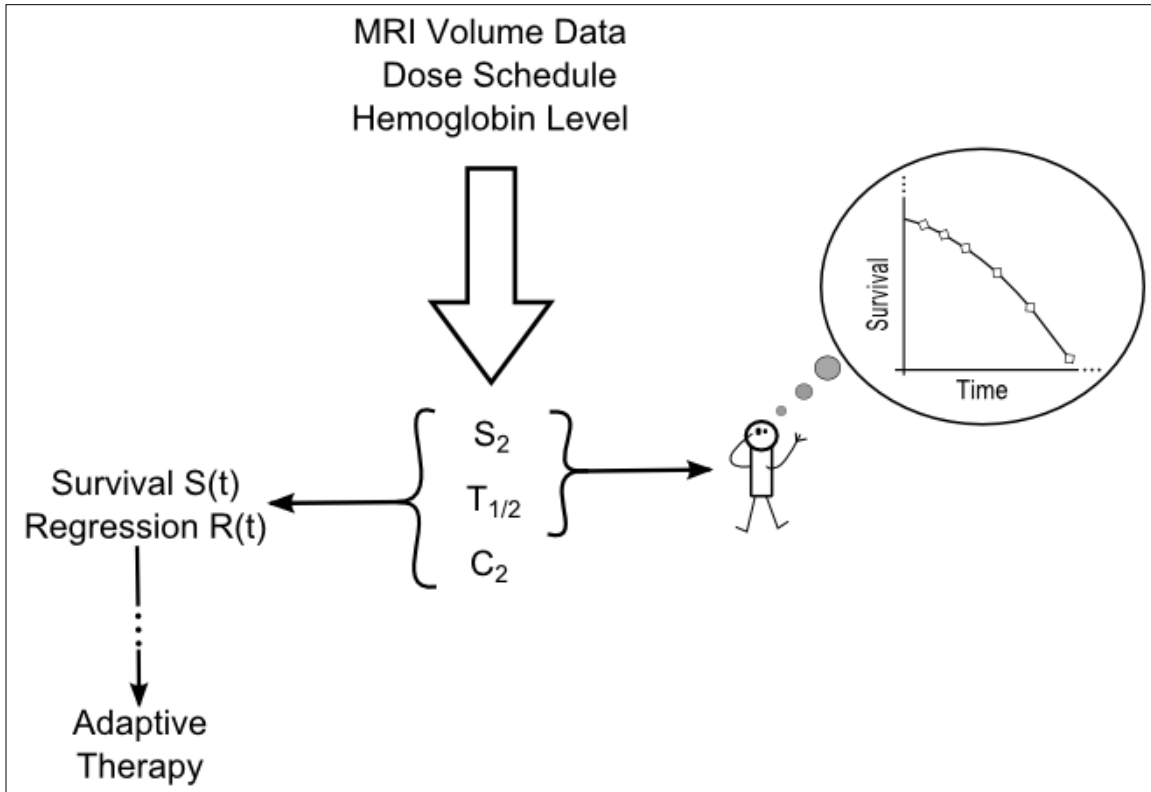
Figure 4. Conceptual Map of Thesis

CHAPTER 2: METHODS

2.1 PATIENT DATA

Modifications to the model are based on data from a population of 78 patients with carcinoma of the cervix who underwent 4 MRI scans throughout the course of treatment. See Appendix B for IRB documentation approving the use of this data.

The patient data used in this thesis is a subset of the patient data used to develop the original model. Patients had stages of cervical cancer ranging from IB up to IVB, and some had locally recurrent tumors. Both squamous cell and adenocarcinomas were represented. The age range of the patients was 25 to 89 years, with a median of 55 years. Each patient underwent a standard treatment plan consisting of pelvic external beam radiation therapy (EBRT) and brachytherapy. EBRT consisted of 45 – 50 Gy total dose delivered in 1.8 – 2.0 Gy fractions. The brachytherapy used 1 – 2 fractions of 20 Gy given at a low dose rate (LDR). 26 of the patients also received cisplatin-based chemotherapy in combination with RT. MRI imaging was performed at the start of RT, at 20 – 25 Gy, at 40 – 45 Gy, and following up 1 – 2 months after treatment. Tumor volumes were precisely delineated on MRI images by radiologists to minimize error.

The preexisting model relies on MRI images and dose schedules as input parameters. Dose delivery schedules are the basis for the volume equations and the use of the index i. The doses administered to patients whose data was later used in this study are as follows:

$$D_i = \begin{cases} 0 & i \text{ represents a day without radiation;} \\ 1.8 \text{ or } 2.0 \text{ Gy} & i \text{ represents a day with EBRT;} \\ D_{LDR} & i \text{ represents a day with LDR brachytherapy.} \end{cases}$$

Where i = 1 represents the first day of RT, and a dose of D_{LDR} is represented in the dose schedule as a value normalized to an EBRT dose in fractions of 1.8 to 2.0 Gy.

For this thesis, average hemoglobin levels were also used as input parameters. These averaged values come from a series of blood tests the patients underwent during the course of treatment. Hemoglobin level data comes from the patients' complete blood count (CBC) and is given in grams per deciliter (g/dL).

Patient data is divided into 2 subgroups based on treatment outcome: the Local Control (LC) subgroup and the Local Failure (LF) subgroup. LF patients either experienced tumor recurrence or had tumors that did not regress in response to therapy. LF includes patient who had died prior to the follow-up time and those who survived but still had cervical cancer at the follow-up time. LC patients had no tumor recurrence at the follow-up time and had tumors that regressed in response to therapy.

2.2 MODIFYING THE MODEL: Incorporating the Oxygen Effect Using Hemoglobin Levels

   The original model is based on three major effects of RT. Those effects are radiation cell killing, tumor repopulation, and dead cell resolving. A goal of this thesis is to incorporate a fourth major effect of RT into the model that (a) works on a similar time scale as the other effects, and (b) is measurable on its own. Requirement (a) is important because analytical solutions to the main model equations will not be truly continuous functions of time (further discussion is provided in section 2.5.2). Requirement (b) is important because it helps to avoid introducing more confounding variables into an already complex system. The oxygen effect meets both requirements (a) and (b). Since exploiting the oxygen effect in RT is based on reoxygenation, the tumor's response to the oxygen effect becomes apparent on a similar timescale timescale as responses to cell-killing, dead cell resolving, and tumor repopulation. Because the oxygen effect has been quantified and well-documented in vitro, it should not act as a confounding variable.

   The oxygen effect not only meets requirements (a) and (b), but is also a highly relevant effect of RT in the living body of a patient. Recall that the Oxygen Enhancement Ratio (OER) is between 2 and 3 for low Linear Energy Transfer (LET) radiation. A well-established principle in medical physics, the oxygen effect has the potential to add meaning and predictive power to the original model. In order to incorporate the oxygen effect into the original model, a qualitative, easily obtainable parameter is needed as an additional form of input data.

   This thesis proposes to use patients' hemoglobin levels as input data to simulate the effect of oxygen during RT. The premise of this idea is based on the fact that red blood cells (RBC) distribute oxygen throughout the body's vasculature [25]. The specific mechanism for this is hemoglobin proteins, which are attached the exterior of the red blood cell, and bind to diatomic

oxygen, so it is carried along with the RBCs. As RBCs are squeezed through capillaries, hemoglobin is released and diffuses into tissue [26]. Though it would be ideal to probe key regions of the tumor to determine local oxygen levels, this is impractical in the clinic. Since hemoglobin levels in this study showed little fluctuation over the course of treatment, the time-average of each patient's hemoglobin levels was used as input data. Hemoglobin level as an index of tumor oxygenation easily meets the requirement for clinical practicality and feasibility.

This approach is not without challenges. While hemoglobin levels correlate highly with well-oxygenated regions of the tumor, they are not representative of hypoxic regions [4]. However, there is considerable evidence in the literature for the correlation between hemoglobin levels and *overall* tumor radiosensitivity, regardless of hypoxic/anoxic regions. W.C. Yuh and colleagues note that radiosensitivity at 2 Gy (S_2) correlates with mean hemoglobin level with a significance of $p = 0.044$ in their 2010 study entitled "Hemoglobin Influences Tumor Cell Radiosensitivity in Patients with Cervical Cancer" [27]. Michelle Grogan and colleagues concluded that "Presenting Hgb [hemoglobin] level, average weekly nadir Hgb (AWNH) during RT, and blood transfusion were correlated significantly with local control, disease free survival, and overall survival on univariate analysis" [28]. A 2012 study by Stephan Walrand and colleagues found a strong correlation ($R = 0.96$) between early response and absorbed dose, and between absorbed dose and hemoglobin levels [29]. The large number of studies demonstrating a correlation between tumor oxygenation and response to radiotherapy prompted the National Cancer Institute to publish recommendations for future research investigating cervical tumors specifically [30]. These publications and many others support the use of hemoglobin levels as an index of tumor oxygenation and a qualitative parameter describing the oxygen effect in RT, especially for cervical cancer.

In this study, hemoglobin levels will be incorporated into the original model with the intent of simulating the oxygen effect simultaneously with the three effects of RT for which the model already accounts. A patient's average hemoglobin level is represented by the variable H_L in the model equations. A scaling constant, C_2, will also be built into the model with H_L. The intended result of C_2 is to improve the fit of the model and to enable specific future investigations (see Discussion section 4.3 for details). The resultant new model will be referred to as "the hemoglobin model" throughout this thesis.

Strategies for including the oxygen effect in the model using hemoglobin levels follow readily from radiobiological principles. The primary result of the oxygen effect is to increase radiation cell killing. That affects tumor volume directly. Consequently, the dead cell volume $V_{d,i}$ should be larger, and the surviving cell volume $V_{s,i}$ should be smaller by the same amount. To simulate this, the volume equations have been modified, resulting in Equations (16) and Equations (17):

$$V_{s,i} = \begin{cases} V_{s,i-1} S_2^{n_i}(1 - C_2 H_L), & \text{when } i \leq T_k, \\ V_{s,i-1} S_2^{n_i} e^{\ln 2/T_d}(1 - C_2 H_L), & \text{when } i > T_k, \end{cases} \quad (16)$$

$$V_{d,i} = \begin{cases} V_{d,i-1} e^{-\ln 2/T_{1/2}} + \left(V_{s,i-1} - V_{s,i}\right) + V_{s,i-1} S_2^{n_i} C_2 H_L & \text{when } i \leq T_k \\ V_{d,i-1} e^{-\ln 2/T_{1/2}} + \left(V_{s,i-1} - V_{s,i}\right) + V_{s,i-1} S_2^{n_i} e^{\ln 2/T_d} C_2 H_L & \text{when } i > T_k \end{cases}$$

$$(17)$$

Equations (16) through (17) were found to optimize the model fit and output parameters better than some simpler modifications. Since these changes shift the proportions of living and dead cells rather than changing the total number of cells, the equation for total volume, Equation (11), and the values for total volume remain unchanged:

$$V_i = V_{s,i} + V_{d,i} \quad (11)$$

Modifications to the volume equations reduce the portion of the tumor volume attributed to surviving cells in order to simulate the oxygen effect in RT. This decrease in surviving cell volume is expected to directly decrease the expected surviving cell fraction over time, $S(t)$. For this reason, the main model equations, Equations (10), are modified as shown in Equations (18):

$$\begin{cases} \frac{dR(t)}{dt} = -\frac{\ln 2}{T_{1/2}}[R(t) - S(t)], \\ \frac{dS(t)}{dt} = S(t)\left[-(1 - S_2) + \frac{\ln 2}{T_d} - C_2 H_L\right] \end{cases} \tag{18}$$

Though the volume equations and main model equations have been modified, Equations (14) and (15) remain the same as in the original model:

$$R_i \cong R(t) \tag{14}$$

$$\begin{cases} R_i = \frac{V_i}{V_0} \\ R(t) = \frac{V(t)}{V(0)} \end{cases} \tag{15}$$

The differences between the hemoglobin model and the original model are summarized in Table 1 below. The expected consequences of how the hemoglobin model will differ from the original model are consistent with how the oxygen effect acts on cells during RT. It is expected that S_2 will decrease, and $T_{1/2}$ may increase or decrease (full discussion of null and alternative hypotheses in section 2.4). Furthermore, it is expected that the additional term will increase mathematical freedom, thus improving the goodness of fit, X^2.

Comparison of Hemoglobin Model and Original Model Equations

Surviving Cell Volume

$$V_{s,i} = \begin{cases} V_{s,i-1}S_2^{n_i}(1 - C_2 H_L), & when\ i \leq T_k, \\ V_{s,i-1}S_2^{n_i}e^{ln2/T_d}(1 - C_2 H_L), & when\ i > T_k, \end{cases}$$

Hemoglobin

$$V_{s,i} = \begin{cases} V_{s,i-1}S_2^{n_i}, & when\ i \leq T_k, \\ V_{s,i-1}S_2^{n_i}e^{\frac{ln(2)}{T_d}}, & when\ i > T_k, \end{cases}$$

Original

Dead Cell Volume

$$V_{d,i} = \begin{cases} V_{d,i-1}e^{-ln2/T_{1/2}} + \left(V_{s,i-1} - V_{s,i}\right) + V_{s,i-1}S_2^{n_i}C_2 H_L & when\ i \leq T_k \\ V_{d,i-1}e^{-ln2/T_{1/2}} + \left(V_{s,i-1} - V_{s,i}\right) + V_{s,i-1}S_2^{n_i}e^{ln2/T_d}C_2 H_L & when\ i > T_k \end{cases}$$

Hemoglobin

$$V_{d,i} = V_{d,i-1}e^{-ln2/T_{1/2}} + \left(V_{s,i-1} - V_{s,i}\right)$$

Original

Main Model

$$\begin{cases} \dfrac{dR(t)}{dt} = -\dfrac{ln2}{T_{\frac{1}{2}}}[R(t) - S(t)], \\ \dfrac{dS(t)}{dt} = S(t)\left[-(1 - S_2) + \dfrac{ln2}{T_d} - C_2 H_L\right] \end{cases}$$

Hemoglobin

$$\begin{cases} \dfrac{dR(t)}{dt} = -\dfrac{ln2}{T_{\frac{1}{2}}}[R(t) - S(t)], \\ \dfrac{dS(t)}{dt} = S(t)\left[-(1 - S_2) + \dfrac{ln2}{T_d}\right] \end{cases}$$

Original

Table 1. Comparison of Hemoglobin Model and Original Model Equations. Blue boxes represent the hemoglobin model. White boxes represent the original model. Note: only the volume equations and main model equations are shown. Equations that are the same for both models are omitted.

2.3 COMPUTING

2.3.1 Numerically Fitting the Output Parameters

To facilitate numerical calculation of the output parameters S_2, $T_{1/2}$, and C_2, a C++ code was developed to perform computations (see Appendix A). The MRI volume data is input into the code as data points of the form $(x, y) =$ (time in days, fraction of original volume remaining). These data points serve as the "true" regression volume ratio values to which the simulated values will be compared. The simulated regression volume ratio values R_i are computed numerically in terms of dose schedule by the code, using the volume equations, Equations (16).

As in the original model, R_i is still a function of time, but it is a step function in dose rather than a (theoretically) continuous function like R(t). The code varies the set of output parameters S_2, $T_{1/2}$, and C_2 within given ranges and compares the resultant R_i for each set to the MRI volume data. After each iteration of the loops that vary S_2, $T_{1/2}$, and C_2, the code selects the set $(S_2, T_{1/2}, C_2)$ that corresponds to the R_i that most closely fits the MRI volume data. The "goodness of the fit" is expressed using the X^2 test statistic, which is also computed by the code. X^2 values provide a gauge of reliability for the output parameters.

S_2 is allowed to vary between 0.2 and 1.0 with a step size of 0.001. $T_{1/2}$ is allowed to vary between 1.5 and 101.5 with a step size of 0.4. C_2 is allowed to vary between 0 and 0.0001 with a step size of 1×10^{-6}. C_2 is not a clinically relevant output parameter like S_2 and $T_{1/2}$; it is included in the interest of obtaining more reliable values for S_2 and $T_{1/2}$ through a better X^2 fit and as a set-up for future studies.

Upon examining Equations (16) – (17), it is noticeable that there are five parameters that could be varied in order to fit R_i to MRI volume data. They are S_2, $T_{1/2}$, C_2, T_d, and T_k. Obvious candidates for variability are S_2 and $T_{1/2}$ because of their relevance in estimating survival curves.

In this study, C_2 is varied for exploratory purposes. This is why S_2, $T_{1/2}$, and C_2 were chosen for variation over T_k and T_d. The fact that average values of T_k and T_d are easily located in the literature on cervical cancer [18-24] solidifies the decision to hold these parameters constant. T_k, the onset time of tumor repopulation, remains constant at 21 days in this study. T_d, effective tumor doubling time after repopulation begins, remains constant at 3.5 days.

It is important to note that S_2, $T_{1/2}$, C_2, and the associated fit, X^2, are obtainable from the model's volume equations alone. The volume equations yield the clinically relevant parameters that comprise the model's most practical usage. To obtain analytic solutions for regression volume ratio R(t) and survival rate S(t) for individual patients, the output parameters S_2, $T_{1/2}$, and C_2 can be taken as constants in the main model equations, which are then solvable. This process is described in greater detail in section 2.5.

2.3.2 Validating Modifications

To ensure that modifications to the model have not resulted in loss of agreement between the volume equations and the main model equations, Equations (14) and (15) are used in a test case to ensure the integrity of the hemoglobin model with respect to the original model. Recall these simple equations:

$$R_i \cong R(t) \tag{14}$$

$$\begin{cases} R_i = \frac{V_i}{V_0} \\ R(t) = \frac{V(t)}{V(0)} \end{cases} \tag{15}$$

The level of agreement between R_i and R(t) for the hemoglobin model should be similar to the level of agreement between R_i and R(t) for the original model. Using the volume equations to get Vi and the analytic solution to the main model equations, R(t), a comparison can be made for any patient at any time t. Methods for obtaining R(t) are discussed in section 2.5. For the purpose of

validating the integrity of the new hemoglobin model, this was done for two patients whose volume data the model was able to fit well with calculated values. The model should be most effective for patients with the best fit between actual volumes and calculated values, i.e., patients whose data produce small X^2 values. Patient 23 and Patient 34 were selected using this criteria. Time t = 18 days was selected randomly for this test, which should work for any time t. Table 2 shows the results.

Model	Patient	V18	R(18)	Difference
Hemoglobin	23	0.24196	0.3837	-0.14174
	34	0.21165	0.2918	-0.08015
Original	23	0.24168	0.3866	-0.14492
	34	0.21137	0.29356	-0.08219

Table 2. Validating modifications of the hemoglobin model

A significant discrepancy between Ri and R(t) can be seen for the both the hemoglobin model and the original model. Since the hemoglobin model does not make the discrepancies of the original model worse, the model changes that resulted in the hemoglobin model are likely not the cause of the discrepancies. The hemoglobin model *changes* are validated by this data, but the models themselves are not. A discussion of likely causes is provided in Discussion section 4.2.

Furthermore, there is only a small difference between predicted R(t) values for the hemoglobin model versus the original model. Incorporating the oxygen effect made only a very small difference. However, the OER is between 2.5 and 3.5, as discussed in Introduction section 1.3.2. This means that the original model already accounts for the oxygen effect to some extent, though that extent has not been quantified.

2.4 INVESTIGATING CLINICAL OUTCOMES: Statistical Analysis of Model Output Parameters

When the oxygen effect in cell killing is incorporated into the model through use of hemoglobin levels, changes to volumetric fit (X^2), tumor cell survival (S_2), and dead cell resolving ($T_{1/2}$) occur. The impact of these changes is quantified using statistical inference. Specifically, the difference-of-means t-test is used to determine whether changes in X^2, S_2, and $T_{1/2}$ are statistically significant. In this case, "significant" means the difference is large enough to be attributed to the hemoglobin term, as opposed to simply being the insignificant result of statistical fluctuation. The idea of inference comes in because it is desirable to know how incorporating the oxygen effect will affect model simulations for the population of cervical cancer patients at large. However, the data available comes from just 78 patients from that population. Since it would be impractical to obtain data on an entire patient population, statistical methods are used which allow the inference of conclusions about the population with reasonable confidence based on sample size, data spread, and other known parameters.

The use of statistical inference techniques imposes certain restrictions. The validity of these methods depends on several characteristics of the population, the sample, and the data collection methods. Measuring the effect of considering the oxygen effect versus not considering it is necessarily a matched pairs study, since each patient's data is subjected to two different methods of analysis, which produces two different-but-dependent data sets. For matched pairs analysis, it is required that

(i)   The sample is a simple random sample (SRS).

(ii)   The data sets are not independent.

(iii)   The sample is taken from a normal or near-normal population [31].

Consider requirement (i): For a sample to be a SRS, it must be such that any given sample of size n is as likely to be chosen as any other sample of size n out of the population. For the group of cervical cancer patients who gave data in this study, a broad range of ages, cancer stages, and medical histories is included so that no specific sub-group is favored. So, (i) is satisfied.

To address requirement (ii), consider that the data sets from the hemoglobin model and the preexisting model are not the same, but they are not independent either, since they were both generated from the same tumor volume data.

Concerning requirement (iii), it would be difficult to comment on the normality of tumor volumes in the entire population of cervical cancer patients. However, the Central Limit Theorem can be invoked in such a way as to approximate a near-normal population scenario using the sample [32]. This is because the distribution of possible *sample means* tends toward normality as the sample size increases. This is true regardless of the shape of the population distribution. A conservative rule of thumb for how large a sample must be in order to invoke the Central Limit Theorem is n > 30, with the condition that there are no extreme outliers in the sample [33].

For convenience, the difference between paired data points for each parameter is defined using Equations (19):

$$d_{\chi^2} = (\chi^2)_P - (\chi^2)_H$$

$$d_{S_2} = (S_2)_P - (S_2)_H \tag{19}$$

$$d_{T_{1/2}} = (T_{1/2})_P - (T_{1/2})_H$$

where the subscript "P" represents the original model, and the subscript "H" represents the hemoglobin model. Similarly, define the difference of *mean* parameter values between the two models using Equations (20):

$$\bar{d}_{\chi^2} = (\overline{\chi^2})_P - (\overline{\chi^2})_H$$

$$\bar{d}_{S_2} = (\overline{S_2})_P - (\overline{S_2})_H \tag{20}$$

$$\bar{d}_{T_{1/2}} = (\overline{T_{1/2}})_P - (\overline{T_{1/2}})_H$$

Difference-of-means analysis uses a hypothesis test as its basis. The null hypothesis H_0 for this study is that there is no difference in the mean X^2, the mean S_2, or the mean $T_{1/2}$ when hemoglobin levels are considered. The alternative hypothesis H_A is that considering hemoglobin levels (a) generates a better fit, i.e., has a smaller X^2, (b) better accounts for tumor cell killing related to the O_2 effect, i.e., has a smaller S_2, and (c) changes dead cell resolving time, i.e., has a different $T_{1/2}$ than the original model. The null hypotheses are expressed in Equations (21) and the alternative hypotheses are expressed in Equations (22):

H_0:

$$(\overline{\chi^2})_H = (\overline{\chi^2})_P \quad or \quad \bar{d}_{\chi^2} = 0$$

$$\bar{d}_{S_2} = 0 \tag{21}$$

$$\bar{d}_{T_{1/2}} = 0$$

H_A:

$$(\overline{\chi^2})_H < (\overline{\chi^2})_P \quad or \quad \bar{d}_{\chi^2} > 0$$

$$\bar{d}_{S_2} > 0 \tag{22}$$

$$\bar{d}_{T_{1/2}} \neq 0$$

Notice that the hypotheses involving X^2 and S_2 are directional. It is expected that both

parameters will be *smaller* for the hemoglobin model. Also note that the alternative hypothesis

for $T_{1/2}$ is non-directional. Biologically speaking, dead cell resolving time could either increase or

decrease due to the oxygen effect. Since more oxygen means a higher metabolic rate, the

clearing away of dead cells may happen faster. On the other hand, the extra cell killing that is

being simulated by the oxygen effect results in a larger dead cell volume that may take longer to

clear away. In is significant to note that this model uses the half-time of dead cell resolving—not

the full time—since dead cell resolving proceeds in an exponential fashion. Therefore, changes

in $T_{1/2}$ are expected to be affected more by increased metabolic rate than by increased dead cell

volume. Ultimately, the direction of the change in $T_{1/2}$ is determined by the more prevalent of the

two effects: increased metabolic rate versus increased dead cell volume.

To test these hypotheses, the matched pairs t-test is used on the means. The t-test statistic

is defined in Equations (23):

$$t = \frac{\bar{d}}{SE}$$

$$SE = \frac{SD}{\sqrt{n}} \quad (23)$$

$$SD = \sqrt{\frac{\sum_i^n d_i^2 - [\frac{(\sum_i^n d_i)^2}{n}]}{n-1}}$$

where SE is standard error on the difference d, SD is standard deviation on the difference d, and

n is sample size [31]. The t-test statistic is compared to a t distribution, which gives the

probability P that t would fall at or below this value, assuming the null hypothesis is true. So,

taking $1 - P$ gives the probability of getting this t-value or higher if the null hypothesis is true.

The simple Equation (24)

$$1 - P = p \quad (24)$$

gives the well-known p-value. For a directional hypothesis, take p as is. For a non-directional hypothesis, a result at the high extreme *or* the low extreme is anticipated, so take p x 2 = p* and use that. In order to evaluate the meaning of p, we must choose some significance level, α, with which to compare p.

If $p \leq \alpha$, then reject the null hypothesis.
If $p > \alpha$, then fail to reject the null hypothesis.

When p is less than or equal to α, it means that the data observed would occur less than five percent of the time for a directional hypothesis and less than 2.5 percent of the time for a non-directional hypothesis, if in fact the null hypothesis were true. This is a conventional basis for rejecting the null hypothesis to conclude the result is significant [32]. When p is greater than α, it means that the data observed would occur by chance more often than five or 2.5 percent of the time, if in fact the null hypothesis were true. In this case, the convention is to fail to reject the null hypothesis and conclude that the result may be due to statistical fluctuation. The choice of significance level is somewhat arbitrary, but this study uses α = 0.05 to determine a significant result. The significance level α = 0.05 is used in the literature on the original model and other patient models [17]. Furthermore, results at the α = 0.05 level are still very appropriate for clinical use, where much greater uncertainty is typical.

Also appearing in this study is the t-test for independent samples, which is used to describe the difference in outcomes from the hemoglobin model between the LC subgroup and the LF subgroup. The test statistic is given in Equation (25):

$$t = \frac{\overline{x_1} - \overline{x_2}}{\sqrt{\dfrac{s_1^2}{n_1} + \dfrac{s_2^2}{n_2}}}$$

(25)

Where $\overline{x_1}$ and $\overline{x_2}$ are the means of the respective samples, s_1 and s_2 are the variances of the respective samples, and n_1 and n_2 are sample sizes [32]. The same rules for determining p-values discussed for the matched pairs t-test apply to this t-test as well.

2.5 INVESTIGATING MATHEMATICAL OUTCOMES: Obtaining Analytical Solutions for Surviving Cell Fraction S(t) and Regression Volume Ratio R(t) using Main Model Equations

Because each patient has a unique S_2 and $T_{1/2}$, analytical solutions to the main model equations are only possible on a patient-by-patient basis. Because the model accounts for cumulative, major effects of RT that take place on the timescale of days rather than faster effects, and because the model is based on a *daily* dose schedule, the applicability of the model is limited to time increments on the order of days. This imposes certain limitations on analytic solutions for R(t) and S(t).

2.5.1   Limiting Factors in the Analytic Solution

It is stated throughout this thesis that the main model equations can be solved for S(t) and R(t). This is based on a few key assumptions. The first assumption is that S_2, $T_{1/2}$, and C_2 are constant over the course of treatment. Their values are obtained computationally by fitting the volume equations to the MRI data. Then, they are simply plugged into the main model Equations (18) like any other constants. The second assumption is that time t is treated as continuous for the purpose of solving the main model equations analytically, but it must be understood that it is not truly continuous in the context of the model.

The body of knowledge on fast cellular and subcellular responses to radiation is well established. If the model were to use increments of time as small as seconds, minutes, or even hours, incorporating these fast processes would be necessary. Sublethal recovery is one such process. Sublethal recovery is the ability of cells to repair minor radiation-induced damage below a certain dose threshold. Sublethal damage is typically repaired by the cell within 2 hours of irradiation [10]. So, the region of the survival curve for hours 0 through 2 is distinctly different than the region of the curve for hours 3 through 24. The stages of radiation action and cellular

response present another timescale complication. Many models of fast processes use stages to classify damage and repair processes by timescale. The physical stage is on the order of 10^{-11} seconds. The physiochemical stage is on the order of 10^{-5} s. The cellular biological stage is on the order of minutes to days. The tissue biological stage is on the order of days to years [34, 35]. While the physical stage and physiochemical stage are not useful for patient models, the cellular biological stage is relevant. The timescales of different radiation response processes vary considerably, making it difficult to simulate processes with different timescales in the same model. To use a time increment of hours or smaller, cell cycle stages must be considered. The four phases of the cell cycle are M (0.5 - 1 hour), G_2 (2 - 4 hours), S (6 - 8 hours), and G_1 (0 hours - very long) [10]. Cell radiosensitivity varies significantly depending on which phase of the cell cycle the cells are undergoing. Another complication comes from the reliance of the hemoglobin model on the theory of tumor reoxygenation. Recall that complete reoxygenation means the proportion of aerated cells has returned to what it was before irradiation. Reoxygenation completes within 24 hours for most mammalian cells, but varies erratically between the time of irradiation and the time at which reoxygenation is finally established [36]. Complicated radiobiological processes present significant difficulties for modeling major effects of RT using time increments smaller than days.

Another reason to use a time increment of days comes directly from fractionated RT dose schedules. It is well known that cell survival is a function of the dose given, and doses are ideally delivered on a daily basis. Surviving fraction S(t) is a function of dose, and fractionated doses are functions of days. Furthermore, the solution for surviving cell fraction S(t) is required to solve for regression volume ratio R(t), so R(t) should employ the same time increment as S(t). Finally, the model is built on the parameters of effective tumor doubling time T_d, and onset time of tumor

repopulation T_k, both of which are given in days. Of course, any decimal value of t could be plugged into the expression R(t); however, for reliable predictions, t must be in increments of days.

2.5.2   Strategy for Solving the Main Model Equations

To obtain the analytic solutions, first recall differential Equations (18):

$$\begin{cases} \frac{dR(t)}{dt} = -\frac{\ln 2}{T_{1/2}}[R(t) - S(t)], \\ \frac{dS(t)}{dt} = S(t)\left[-(1 - S_2) + \frac{\ln 2}{T_d} - C_2 H_L\right] \end{cases} \tag{18}$$

Because the first of Equations (18) expresses the dependence of R(t) on S(t), S(t) is determined first. Begin by defining the bracketed term in the bottom equation as "a" for convenience:

$$a \stackrel{\text{def}}{=} -(1 - S_2) + \frac{\ln 2}{T_d} - C_2 H_L \tag{A}$$

It can be seen that the bottom equation is a separable differential equation of the first order. It has the following general solution:

$$S(t) = e^{at + K_1} \tag{B}$$

where K_1 is a constant of integration. Using the initial condition that $S(t=0) = 1$, it can be determined that K_1 must be equal to 0. So, the final solution is:

$$S(t) = e^{at} \tag{C}$$

Next, consider the first of Equations (18). For convenience, define the coefficient on the right hand side as "b":

$$b \stackrel{\text{def}}{=} \frac{\ln 2}{T_{1/2}} \tag{D}$$

Now, plugging in b and the solution for S(t), the equation becomes:

$$\frac{dR(t)}{dt} = -b[R(t) - e^{at}] \tag{E}$$

As Z. Lin notes, the solution will be of the form:

$$R(t) = n_1 + n_2 e^{-bt} + n_3 e^{at} \qquad [F]$$

where n_1, n_2, and n_3 are constants, and

$$R'(t) = -bn_2 e^{-bt} + an_3 e^{at} \qquad [G]$$

Substituting R(t) and R'(t) back into the expression for dR(t)/dt and comparing terms on either side of the equation, two constants can be determined:

$$\begin{cases} n_1 = 0 \\ n_2 = \text{undetermined} \\ n_3 = \dfrac{b}{a+b} \end{cases} \qquad [H]$$

n_2 can be found using the initial condition that R(t=0)=1. The resultant expression for n_2 is:

$$n_2 = \frac{a}{a+b} \qquad [I]$$

Simple resubstitution of the constants determined into the expression [E] will give the analytic solution for R(t). Both S(t) and R(t) are reported in terms of the convenient constants a and b, and in terms of the model constants S_2, $T_{1/2}$, C_2, H_L, T_d, and T_k in Results section 3.2.

CHAPTER 3: RESULTS

This study results in a dual outcome. Section 3.1 reports on the significance of changes in X^2, S_2 and $T_{1/2}$ that have resulted from incorporating hemoglobin levels into the model to simulate the oxygen effect. This is considered the clinical outcome. Section 3.2 reports on the analytic solutions $S(t)$ and $R(t)$—the mathematical outcome.

3.1 CLINICAL OUTCOMES: Model Output Parameters

The following statistics are based on t-tests of statistical significance for differences between means, including the matched-pairs t-test for dependent data sets and the t-test for independent samples (discussed in Methods section 2.5). The patient data consisting of MRI-determined tumor volumes, dose schedules, and average hemoglobin levels was subjected to two different treatments—the original model and the hemoglobin model—to produce two different sets of outcome parameters X^2, S_2, and $T_{1/2}$. Those sets of parameters are compared to determine the significance of the differences between the two models. Results are shown for the overall patient group and for the subgroups of Local Control (LC) patients and Local Failure (LF) patients. Recall from chapter 2 that patient data is divided into 2 subgroups based on treatment outcome: the Local Control (LC) subgroup and the Local Failure (LF) subgroup. LF patients either experienced tumor recurrence or had tumors that did not regress in response to therapy. LC patients had no tumor recurrence at the follow-up time and had tumors that did regress in response to therapy. To determine if the hemoglobin model affects the LC subgroup and the LF subgroup differently, significance test results are provided for difference in X^2, S_2, and $T_{1/2}$ between the two subgroups. The significance level $\alpha = 0.05$ is the comparison criterion for determining whether or not a result is considered significant.

A summary of the raw output data for X^2, S_2, and $T_{1/2}$ from both models is provided in Table 3. The model parameters are categorized according to patient group. "N" is number of data points, or patients who gave data. "DF" is degrees of freedom. "SD" is standard deviation, and "SE on Mean" is the standard error on the mean.

Patient Group	Model Parameter	Model	N	DF	Mean	SD	SE on Mean
Overall	**X2**	Original	78	77	212.48	318.07	36.014
		Hemoglobin	78	77	206.11	316.62	35.851
	S2	Original	78	77	0.5998	0.19019	0.02153
		Hemoglobin	78	77	0.6035	0.19214	0.02176
	T1/2	Original	78	77	16.11	11.07	0.02153
		Hemoglobin	78	77	16.213	11.092	0.02176
Local Control (LC)	**X2**	Original	60	59	185.9	296.91	38.331
		Hemoglobin	60	59	185.07	296.27	38.248
	S2	Original	60	59	0.5824	0.19235	0.02483
		Hemoglobin	60	59	0.5835	0.19305	0.02492
	T1/2	Original	60	59	12.713	6.3498	0.02483
		Hemoglobin	60	59	12.68	6.3432	0.02492
Local Failure (LF)	**X2**	Original	18	17	301.08	376.12	88.651
		Hemoglobin	18	17	276.25	377.73	89.032
	S2	Original	18	17	0.6577	0.17553	0.04137
		Hemoglobin	18	17	0.6699	0.17833	0.04203
	T1/2	Original	18	17	27.433	15.447	0.04137
		Hemoglobin	18	17	27.989	15.058	0.04203

Table 3. Summary of raw output data from original model and hemoglobin model.

Small difference in average values of X^2, S_2, and $T_{1/2}$ exist between the original model and the hemoglobin model within each group. Table 4 summarizes the results of matched-pairs t-tests of significance for these differences.

Patient Group	Model Parameter	N	Difference in Means	t-statistic	p-value
overall	X2	78	6.367	1.211	0.1145
	S2	78	-0.00371	1.36	0.911
	T1/2	78	-0.10256	0.618	0.539
Local Control (LC)	X2	60	0.823	5.22	0.00000122
	S2	60	-0.00115	2.735	0.996
	T1/2	60	0.0333	2.316	0.024
Local Failure (LF)	X2	18	24.829	1.093	0.145
	S2	18	-0.01222	1.04	0.8435
	T1/2	18	-0.55556	0.768	0.453

Table 4. Summary of significance tests for comparing the original model output and the hemoglobin model output. Difference = Original Model parameter – Hemoglobin Model parameter.

Small p-values indicate that the data observed in this work would be very unlikely to occur if in fact there was no significant difference in the model output parameters produced by the original model versus the hemoglobin model. Specifically, p-values smaller than 0.05 are considered small enough to be significant. They indicate that if the null hypothesis (of no difference) were true, then, at most, 5% of samples from the population would show this type of data.

Overall Patient Group

The hemoglobin model does not produce statistically significant changes in fit (X^2), survival at 2 Gy (S_2), or half-time of dead cell resolving ($T_{1/2}$) when compared to the original model. Though the mean X^2 is smaller for the hemoglobin model than for the original model, the decrease is not statistically significant. Similarly, the mean S_2 and $T_{1/2}$ are very slightly larger for the hemoglobin model than the original model, but these increases are not deemed significant using t-test methods.

Local Control Patient Group

The hemoglobin model produces significant changes in fit (X^2) and half-time of dead cell resolving ($T_{1/2}$) when compared to the original model. The high t-values and correspondingly low p-values for differences in X^2 and $T_{1/2}$ fall below the $\alpha = 0.05$ significance level, so it is safe to reject the null hypothesis that there is no difference in these parameters between the two models. This indicates that the incorporation of the hemoglobin term simulates a faster half-time for dead-cell resolving, $T_{1/2}$, in accordance with the radiobiological principle that well-oxygenated cells metabolize waste faster. The hemoglobin model does not produce significant changes in survival at 2 Gy (S_2) for this group. Though mean S_2 is slightly higher for the hemoglobin model, the difference is not significant.

Local Failure Patient Group

The hemoglobin model does not produce statistically significant changes in fit (X^2), survival at 2 Gy (S_2), or half-time of dead cell resolving ($T_{1/2}$) when compared to the original model. For the hemoglobin model, mean X^2 is smaller, and mean S_2 and mean $T_{1/2}$ are larger, but none of these differences are statistically significant.

The results of the matched-pairs t-tests for significance indicate that the hemoglobin model resulted in significant changes to output parameters for the Local Control patient group. However, changes were not significant for the overall patient group or the Local Failure patient group. To quantify the different effect the hemoglobin model may have on the LC and LF subgroups, t-tests for independent samples were performed. Table 5 summarizes the results of those tests.

Output Parameter	Levene's F	F Significance	Equal Variance?	DF	t-statistic	p-value	Mean Difference	SE on Difference
X2	0.573	0.452	Y	76	1.073	0.857	-91.181	85.007
S2	2.047	0.157	Y	76	1.693	0.9527	-0.0863556	0.05102
T1/2	20.96	0	N	18.8	4.203	0.000534	-15.3089	3.6424

Table 5. Summary of significance tests for comparing the hemoglobin model LC output and the hemoglobin model LF output. Difference = Original Model parameter – Hemoglobin Model parameter.

The p-value for the magnitude of change to $T_{1/2}$ caused in the LC group compared to the magnitude of change to $T_{1/2}$ caused in the LF group is statistically significant. It can be concluded that the hemoglobin model affects the LC group differently than it affects the LF group. The difference in effect between the two patient subgroups for X^2 and S_2 are not significant.

3.2 MATHEMATICAL OUTCOMES: Analytic Solutions for Surviving Cell Fraction S(t) and Regression Volume Ratio R(t)

The mathematical outcome of this thesis is the analytic solution for surviving cell fraction S(t) and regression volume ratio R(t), where both are functions of time, and time is expressed in number of days into treatment. As previously stated, S_2, and $T_{1/2}$ are numerically fitted values from the volume equations simulated using the code, and they are treated as constants. T_k, the onset time of tumor repopulation, and T_d, the effective tumor doubling time after repopulation begins, are held fixed at 21 and 3.5 days, respectively, throughout this study. Equations (26) below were obtained from solving the main model Equations (18).

$$\begin{cases} S(t) = e^{\left[-(1-S_2)+\frac{\ln 2}{T_d} - C_2 H_L\right]t}, \\ R(t) = \dfrac{1}{-(1-S_2)+\frac{\ln 2}{T_d} - C_2 H_L + \frac{\ln 2}{T_{1/2}}}\left\{\left[-(1-S_2)+\frac{\ln 2}{T_d} - C_2 H_L\right]e^{-\frac{\ln 2}{T_{1/2}}t} + [\frac{\ln 2}{T_{1/2}}]e^{\left[-(1-S_2)+\frac{\ln 2}{T_d} - C_2 H_L\right]t}\right\} \end{cases}$$

$$(26)$$

Equations (26) can be expressed more succinctly by Equations (26*) below:

$$\begin{cases} S(t) = e^{at}, \\ R(t) = \frac{1}{a+b}[ae^{-bt} + be^{at}] \end{cases}$$

where $(26*)$

$$a = -(1-S_2) + \frac{\ln 2}{T_d} - C_2 H_L$$

$$b = \frac{\ln 2}{T_{1/2}}$$

A complete analytic solution for regression volume ratio R(t) demonstrates agreement with the volume equations. Using the strategy of equation R(t) and R_i for any arbitrarily selected time, this completeness of the analytic solution can be tested. If Equations (26*) are a complete

solution, $R(t)$ and R_i will be close in value. Patient 23 and Patient 34 were selected to test Equations (26*). The randomly selected time was day 18 of treatment. The results are given in Table 6.

Patient	R18	R(18)
23	0.24196	0.3834
34	0.21165	0.2920

Table 6. Testing R_i and $R(t)$ agreement.

$R(t)$ is considerably larger than R_i for both patients. Even though $R(t)$ is a correct solution to the main model differential equations, $R(t)$ and R_i are not close in value. Several possible reasons for this discrepancy and potential solutions are presented in Discussion sections 4.2 and 4.3

CHAPTER 4: DISCUSSIONS

4.1 DISCUSSING CLINICAL OUTCOMES

Overall Patient Group

For the overall patient group, no changes in X^2, S_2, and $T_{1/2}$ caused by the hemoglobin model are statistically significant. The changes observed in X^2, S_2, and $T_{1/2}$ support the null hypotheses of the t-tests performed. Using the hemoglobin model, this study is able to incorporate the oxygen effect as a fourth effect of RT through an additional variable H_L and scaling parameter C_2 without loss of goodness of fit or output parameter integrity for the overall patient group.

Local Control Patient Group

For the Local Control patient group, changes in X^2 and $T_{1/2}$ caused by the hemoglobin model are statistically significant. The changes in X^2 and $T_{1/2}$ support the alternative hypotheses consistent with the hypothesis and specific aims of this thesis. The fact that the half-time of dead cell resolving, $T_{1/2}$, significantly decreased indicates that the increased cell metabolism simulated by the oxygen effect is more influential than the increased dead cell volume, answering the questions posed in the null hypotheses of Methods section 2.4. Changes in S_2 however, are insignificant, and support the null hypothesis of the t-test for changes in S_2. Using the hemoglobin model, this study is able to incorporate the oxygen effect as a fourth effect of RT through an additional variable H_L and scaling parameter C_2 while improving the model fit and output parameter integrity for $T_{1/2}$ for the LC patient group.

Local Failure Patient Group

For the Local Failure patient group, no changes in X^2, S_2, and $T_{1/2}$ caused by the hemoglobin model are statistically significant. The changes observed in X^2, S_2, and $T_{1/2}$ support

the null hypotheses of the t-tests performed. Using the hemoglobin model, this study is able to incorporate the oxygen effect as a fourth effect of RT through an additional variable H_L and scaling parameter C_2 without loss of goodness of fit or output parameter integrity for the overall patient group.

Of the three patient groups analyzed, only the LC group confirmed the thesis hypothesis that incorporating the oxygen effect into the model as another major effect of RT would improve goodness of fit or significantly change output parameter values. Since the LC group is characterized by its responsiveness to RT, this result is unsurprising. It can be concluded that the hemoglobin model is more powerful when used for patients whose tumors behave ideally in response to therapy. This conclusion is further supported by the significance tests for comparing the hemoglobin model LC output and the hemoglobin model LF output, as summarized in chapter 3 Table 4. Ultimately, the thesis hypotheses that X^2 would decrease and $T_{1/2}$ would change were proven for the LC group, but not the LF group or the overall group.

None of the three patient groups showed the hypothesized decrease in S_2. Since the oxygen effect increases cell killing due to RT, this is a problematic result. Even at the low dose of 2 Gy, a decrease in survival is expected. There are several possible reasons that S_2 did not decrease for the hemoglobin model. One possible cause of S_2 trends seen in the hemoglobin model is the way H_L and C_2 were incorporated into the main model equations. Recall the analytic solution S(t) to the main model equation for dS(t)/dt from Equations (26) and (26*):

$$S(t) = e^{\left[-(1-S_2) + \frac{\ln 2}{T_d} - C_2 H_L\right]t} = e^{at} \qquad (26\text{-}26^*)$$

For this solution, as the constant "a" increases, S(t) decreases. It is true that the hemoglobin model S(t) is smaller than the original model S(t) because the original model does not contain the "$-C_2 H_L$" term. However, for a fixed S(t), subtracting off the hemoglobin term

drives up S_2. A worthwhile future investigation would be to incorporate the hemoglobin term C_2H_L in such a way that it does not directly compete with S_2 in the exponent. Another possible explanation for the behavior of S_2 is that combination of RT and chemotherapy are confounding variables when it comes to cell killing. Recall that 26 patients received both forms of therapy. The model only accounts for RT cell killing, but certainly chemotherapy contributes to cell killing as well. A third possible explanation for the S_2 trends observed in this study refers to the Target Model for cell survival described in chapter 1. The survival curve's shoulder width is described by D_q [10]. If D_q is greater than 2 Gy, then increased cell killing may not be apparent at that dose because of sublethal repair of radiation damage. However, increased cell killing would still be apparent at higher doses. This explanation is testable by plotting analytic $S(t)$ values for time points corresponding to a range of doses for each model, and then comparing the survival curves.

4.2 DISCUSSING MATHEMATICAL OUTCOMES

Chapter 3 Table 5 indicates a considerable discrepancy between the regression volume ratio predictions R(t) and R_i. There are two likely reasons for this. First, the main model equations don't account for lapses in fractionated RT therapy that typically occur on weekends. These lapse periods should technically have unique expressions $S_L(t)$ and $R_L(t)$ rather than using S(t) and R(t). Two days of RT theoretically should not have the same cell surviving fraction and regression volume ratio as two days without treatment. The second likely reason for the discrepancy is that the main model equations don't account for onset time of tumor repopulation T_k, and the volume equations do account for it. A solution to this problem is to break up all analytic solutions S(t), $S_L(t)$, R(t), and $R_L(t)$ into conditional expressions based on whether or not $t > T_k$, as in the volume equations (16) and (17). An analytic solution addressing both these issues is possible, using a step function in dose days of conditional expressions in t, as shown below in Equations (27):

$$S_c(t) = \left|_{t=i_1}^{t=i_n} \begin{cases} S(t), & t \leq T_k \\ S_{repop}(t), & t > T_k \end{cases} \right. + \left|_{i_{n+1}}^{i_{n+1+m}} \begin{cases} S_L(t), & t \leq T_k \\ S_{L,repop}(t), & t > T_k \end{cases} \right.$$

$$+ \left|_{i_{n+2+m}}^{i_{n+2+m+n'}} \begin{cases} S(t), & t \leq T_k \\ S_{repop}(t), & t > T_k \end{cases} \right. + \left|_{i_{n+3+m+n'}}^{i_{n+3+m+n'+m'}} \begin{cases} S_L(t), & t \leq T_k \\ S_{L,repop}(t), & t > T_k \end{cases} \right. + \cdots$$

$$R_c(t) = \left|_{t=i_1}^{t=i_n} \begin{cases} R(t), & t \leq T_k \\ R_{repop}(t), & t > T_k \end{cases} \right. + \left|_{i_{n+1}}^{i_{n+1+m}} \begin{cases} R_L(t), & t \leq T_k \\ R_{L,repop}(t), & t > T_k \end{cases} \right.$$

$$+ \left|_{i_{n+2+m}}^{i_{n+2+m+n'}} \begin{cases} R(t), & t \leq T_k \\ R_{repop}(t), & t > T_k \end{cases} \right. + \left|_{i_{n+3+m+n'}}^{i_{n+3+m+n'+m'}} \begin{cases} R_L(t), & t \leq T_k \\ R_{L,repop}(t), & t > T_k \end{cases} \right. + \cdots$$

where S(t) and R(t) described therapy days, $S_L(t)$ and $R_L(t)$ describe lapse days, the subscript "repop" means the expression accounts for the onset of tumor repopulation, and the subscript "c" stands for "complete," as in, "a complete solution." The indices i are treatment days, and the indices j are lapse days. n is the number of consecutive treatment days at the beginning of RT, n' is the number of consecutive treatment days after the first lapse, n'' would be the number of consecutive treatment days after the second lapse, and so on. Similarly, m is the number of consecutive days of the first lapse, m' is the number of consecutive days of the second lapse, and so on. This type of solution would address inadequacies of analytic solutions S(t) and R(t) as given in equations (26) and (26*); but, it is much more mathematically cumbersome. However complex, these time-dependent analytic expressions have great potential to contribute to treatment plans that are both customized and adaptive.

4.3 FUTURE DIRECTIONS FOR RESEARCH

The above discussions of the clinical and mathematical outcomes of this study motivate several directions for future research. Reinvestigating the strategy for incorporating the hemoglobin variable H_L and scaling term C_2 into the main model equations may improve the model's ability to simulate the change in S_2 caused by incorporating the oxygen effect. The main model equations reflect the change using a linear relationship between S_2 and H_L, while the volume equations reflect the change using a multiplicative relationship between S_2 and H_L. This inconsistency is not easily resolved within the confines of the model equations. A way to modifiy the model that is more consistent between the main model equations and the volume equations is a useful future step. Perhaps the most crucial extension of this study is the determination of the expressions in Equations (27). Cell surviving fraction and regression volume ratio for lapse times, $S_L(t)$ and $R_L(t)$, are needed. Additionally, $S(t)$, $R(t)$, $S_L(t)$, and $R_L(t)$ each need a corresponding repopulation expression for the bracketed equations sets. Development of the complete analytic solutions $S_c(t)$ and $R_c(t)$ is a major milestone to strive for in further development of this kinetic model.

As mentioned previously, the original model already simulates the oxygen effect to some extent. The low S_2 values produced by the original model indicate this is the case. An important future direction for research involving the hemoglobin model is to quantify the extent to which the original model simulates the oxygen effect. It would be ideal to have separate terms accounting for direct radiation cell-killing and the indirect action of the oxygen effect. This would enable more in-depth studies involving different mechanisms of radiation cell killing.

In addition to improving the hemoglobin model as described above, future directions in research can now use the hemoglobin model to simulate the effect of changing blood oxygen

content on tumor shrinkage. There is an abundance of discussion in the oncology literature on the effect of blood oxygen levels and anemia on tumor response to RT [30, 36]. The hemoglobin model is poised to investigate those questions from a mathematical standpoint.

Another future direction for development of the hemoglobin model is to account for hypoxic fractions, which can be estimated from MRI images. This refinement of the oxygen effect within the model could improve accuracy and address a topic that is important in treatment planning.

Finally, just as the original model becomes the hemoglobin model in this study, perhaps the hemoglobin model could become the "hemoglobin + fifth effect" model. Good candidates for the fifth effect of RT will be dose-dependent and tumor repopulation-dependent. For example, there is evidence that tissue acidosis, measureable in terms of blood pH, is a predictor of therapy outcomes [4].

Though development of *in vivo* patient models like the hemoglobin model presented in this thesis presents many challenges, the potential of these models to produce further insight into pressing and relevant topics in oncology makes them a worthy investment of research resources.

REFERENCES

[1]   **FAQs: SBRT**. *Radiation Oncology UCLA.com*. UCLA Health. Web. 25 March 2014.

[2]   **Cervical Cancer Survival Statistics.** *Cancer Research UK.com*. Cancer Research UK, 3 September 2012. Web. 25 March 2014.

[3]   Huang, Zhibin, Nina A. Mayr, Simon S. Lo, and William Yuh. **Radiobiology of Stereotactic Body Radiation Therapy.** *Clinical Insights*. Future Medicine Ltd., 2013. 19-37. doi:10.2217/EBO.13.13

[4]   Vaupel, Peter, Friedrich Kallinowski, and Paul Okunieff: **Blood Flow, Oxygen and Nutrient Supply, and Metabolic Microenvironment of Human Tumors: A Review.** *Cancer Research*. 49, 6449-6465 (1989).

[5]   Rockwell, Sara. **Experimental Radiotherapy: A Brief History.** *Radiation Research*. 150(5), S157-S169 (1998).

[6]   Hall, Eric J., and Amato J. Giaccia. **Radiobiology for the Radiologist.** Philadelphia: *Lippincott Williams and Wilkins*, 2006. Print.

[7]   Moulder, J. E., and S. Rockwell. **Hypoxic Fractions of Solid Tumors: Experimental Techniques, Methods of Analysis, and a Survey of Existing Data.** *International Journal of Radiation Oncology*Biology*Physics*. 10, 695-712 (1984).

[8]   Van Putten, L. M., and R. F. Kallman. **Oxygenation Status of a Transplantable Tumor During Fractionated Radiotherapy**. *Journal of the National Cancer Institute*. 40, 441-451 (1968).

[9]   **Radical (chemistry).** *Wikipedia*. Wikimedia Foundation, Inc. Web. 10 March 2014.

[10]   Biaglow, John E. **The Effects of Ionizing Radiation of Mammalian Cells.** *Journal of Chemical Education*. 58(2), 144-156 (1981).

[11]   Quintiliani, M. **Review: The Oxygen Effect in Radiation Inactivation of DNA and Enzymes**. *The International Journal of Radiation Biology*. 50(4), 573-594 (1986).

[12]   **Chemical Monitoring and Management: Human Activity and the Atmosphere**. *The Northeast ALS Consortium*. Web. 10 March 2014.

[13]   Adelman, R., R. L. Saul, and B. N. Ames. **Oxidative Damage to DNA: Relation to Species Metabolic Rate and Life Span.** *Proceedings of the National Academy of Sciences of the United States of America*. 85(8), 2706-2708 (1988).

[14]   Whitmore, G.F. **One Hundred Years of X Rays in Biological Research**. *Radiation Research*. 144(2), 148-159 (1995).

[15] Schreiber, Gary J. **General Principles of Radiation Therapy**. *Medscape*, 2013. Web. 14 March 2014.

[16] Puck, Theodore T., and Philip I. Marcus. **Action of X-Rays on Mammalian Cells.** *The Journal of Experimental Medicine*. 103(5), 653-666 (1956).

[17] Huang, Zhibin, Nina A. Mayr, William T. C. Yuh, Simon S. Lo, Joseph F. Montebello, John C. Grecula, Lanchun Lu, Kaile Li, Hualin Zhang, Nilendu Gupta, and Jian Z. Wang. **Predicting Outcomes in Cervical Cancer: A Kinetic Model of Tumor Regression during Radiation Therapy.** *Cancer Research*. 70(2), 463-470 (2010).

[18] Symonds, P., B. Bolger, D. Hole, J. H. Mao, and T. Cooke. **Advanced-Stage Cervix Cancer: Rapid Tumor Growth Rather Than Late Diagnosis.** *British Journal of Cancer*. 83, 566-568 (2000).

[19] Hill, RP, W. Fyles, M. Milosevic, M. Pintilie, and R. W. Tsang. **Is There a Relationship Between Repopulation and Hypoxia/Reoxygenation? Results from Human Carcinoma of the Cervix**. *International Journal of Radiation Oncology*Biology*Physics*. 79, 487-494 (2003).

[20] Trott, K. R., and J. Kummermehr. **What is Known About Tumour Proliferation Rates to Choose Between Accelerated Fractionation or Hyperfractionation?** *Radiotherapy & Oncology*. 3, 1-9 (1985).

[21] Bolger, B. S., R. P. Symonds, P. D. Stanton, A. B. MacLean, R. Burnett, P. Kelly, and T. G. Cooke. **Prediction of Radiotherapy Response of Cervical Cancer Carcinoma Through Measurement of Proliferation Rate.** *British Journal of Cancer*. 74, 1223-1226 (1996).

[22] Tsang, T. W., S. Juvet, M. Pintilie, R. P. Hill, C. S. Wong, M. Milosevic, W. Chapman, W. Levin, L.A. Manchul, and A. W. Fykes. **Pretreatment Proliferation Parameters Do Not Add Predictive Power to Clinical Factors in Cervical Cancer Treated with Definitive Radiation Therapy.** *Clinical Cancer Research*. 9, 4387-4395 (2003).

[23] Wigg, D.R. **Applied Radiobiology and Bioeffect Planning.** Madison, Wisconsin: *Medical Physics Publishing*, 2001.

[24] Roberts, S.A., and J. H. Hendry. **The Delay Before Onset of Accelerated Tumor Cell Repopulation During Radiotherapy: a Direct Maximum-likelihood Analysis of a Collection of Worldwide Tumor-control Data.** *Radiotherapy & Oncology*. 29, 69-74 (1993).

[25] **Red Blood Cell**. *Wikipedia*. The Wikimedia Foundation, Inc. Web. 1 April 2014.

[26] **Hemoglobin**. *Wikipedia*. The Wikimedia Foundation, Inc. Web. 1 April 2014.

[27]   W.C. Yuh, Z. Huang, N. A. Mayr, S. S. Lo, G. Jia, J. C. Grecula, and J.Z. Wang. **Hemoglobin Influences Tumor Cell Radiosensitivity in Patients with Cervical Cancer.** Abstract 254 from *Proceedings of the 52nd Annual ASTRO Meeting* 2010: San Diego. S119 (2010).

[28]   Grogan, Michelle, Gillian M. Thomas, Iris Melamed, Frances L. W. Wong, Robert G. Pearcey, Paul K. Joseph, Lorraine Portelance, Juanita Cook, and Keith D. Jones. **The Importance of Hemoglobin Levels during Radiotherapy for Carcinoma of the Cervix.** *Cancer*. 86(8) 1528-1536 (1999).

[29]   Walrand, Stephan, Renaud Lhommel, Pierre Goffette, Marc Van den Eynde, Stanislas Pauwels, and Francois Jamar. **Hemoglobin Level Significantly Impacts the Tumor Cell Survival Fraction in Humans After Internal Radiotherapy.** *EJNMMI Research*. 2(20), 1-8 (2012). doi:10.1186/2191-219X-2-20

[30]   Stone, Helen B., J. Martin Brown, Theodore L. Phillips, and Robert M. Sutherland. **Oxygen in Human Tumors: Correlations between Methods of Measurement and Response to Therapy: Summary of a Workshop Held November 19-20, 1992, at the National Cancer Institute, Bethesda, Maryland.** *Radiation Research*. 136(3), 422-434 (1993).

[31]   **Hypothesis Test: Difference Between Paired Means.** *Stat Trek*. Web. 2 January 2014.

[32]   Moore, David S., George P. McCabe, and Bruce A. Craig. **Introduction to the Practice of Statistics.** New York: *W.H. Freeman and Company*, 2009.

[33]   **Sampling Distributions**. *Stat Trek*. Web. 3 January 2014.

[34]   Kucková, S. **Mathematical Modelling of Radiobiological Effect of Oxygen.** *WDS '05 Proceedings of Contributed Papers*. Part I, 185-189 (2005).

[35]   Adams, G. E., and D. G. Jameson. **Time Effects in Molecular Radiation Biology.** *Radiation and Environmental Biophysics*. 17, 95-113 (1980).

[36]   Rockwell, S., and J. E. Moulder. **Biological Factors of Importance in Split-Course Radiotherapy.** *Optimization of Cancer Radiotherapy*. 171-182 (1985)

APPENDIX A: C++ CODE FOR HEMOGLOBIN MODEL

```cpp
#include <fstream>
#include <iomanip>
#include <assert.h>
#include <math.h>
#include <iostream>
#include <stdlib.h>
using namespace std;


int main(void)
{
        ifstream infp1, infp2, infp3;
        infp1.open("dose_time.dat",ios::in);
        infp2.open("vol_time.dat",ios::in);
        infp3.open("hemoglobin.dat",ios::in);
        assert(infp1);
        assert(infp2);
        assert(infp3);

        ofstream outfp1, outfp2;
        outfp1.open("out.dat",ios::out);
        outfp2.open("vol_change.dat",ios::out);
        assert(outfp1);
        assert(outfp2);
        outfp1 << setiosflags(ios::right);
        outfp1 << setiosflags(ios::fixed | ios::showpoint) << setprecision(4);
        //outfp1 << setiosflags(ios::scientific | ios::showpoint) << setprecision(4);
        outfp2 << setiosflags(ios::right);
        outfp2 << setiosflags(ios::fixed | ios::showpoint)  << setprecision(4);

        int i,j,jj,k,m,n, nday=250;
        int i0,j0,m0,n0;
        double sf, ht, eta, t, rate1[300], rate2[300], aa,bb,cc,dd,ee, dose1[300];
        double dose[300],vol[300],v1[300],v2[300],vom[300],va[300],vb[300];

        int day0[4];
        double vol1[4],sv1[4],vol2[4],sd2[4]],vol11[4],vol1s[4];

        double doubleTime1, doubleTime10 = 2.; // doublling time of prolif. (day)
        double prolifRate;

        double chi, chi2, chi0;

        for (i=1; i<300; i++)
```

```
    {dose[i] = 0.0;
     dose1[i]=0.0
            //vom[i] = 0.0;
     }

    for (i=1; i<90; i++)
     {
     infp1>>j>> dose[i];
     if (infp1.eof())break;
     }

    for (i=1;i<100; i++)
     {
     count << "i=  " << i << "   dose= " << dose{i} << endl;
     }

            for (i=0; i<4; i++)
            {
            infp2 >> day0{i} >> vol2[i] >> sd2[i] >> vol1[i] >> sd1[i];
            cout << ds1[i] << endl;
            vol11[i]=0.0;
            }

double hemo1, hemo10 = 10.0;
for (i=1; i<2; i++)
        {
        infp3 >> hemo10;
        if (infp3.eof( )) break;
        }

double sf1, sf10 = 0.2;
double sf2, sf20 = 0.4;
double resoTime1, resoTime10 = 8.0;
double resoTime2, resoTime20 = 8.0;

chi0 = 100000000.0;

for (m=0; m<800; m++)
        {
        sf1 = sf10 + m/1000.0;

         for (n=0; n<nday; n++)
        {
        resoTime1 = 1.5 + resoTime10*n/20.;

        for (jj=0; jj<100;jj++)
```

```c
{
hemo1 =   jj/1000000.0;

 for (j=0; j<1; j++)
{
doubleTime1 = 3.5;
prolifRate = exp(log(2.0)/doubleTime1);

vol[0] = 1.0;
v1[0] = 1.0;
v2[0] = 0.0;

for (i=1; i<nday+1; i++)
{
eta = log(2.0)/resoTime1;
aa = dose[i]/1.8;

        if (i<22)
        {
        v1[i]=v1[i-1]*pow(sf1,aa)*(1-hemo1*hemo10); //corresponds to volume
equations in hemoglobin model
        }
```
/* Tk= 21 days, where Tk is the onset time of tumor repopulation for cervical cancer. This value
is from the literature. So, for the case where the day corresponds to less than 22, we calculate the
expected tumor volume as shown above. */
```c
        else
        {
        v1[i]=v1[i-1]*pow(sf1,aa)*prolifRate*(1-hemo1*hemo10);  //corresponds
to volume in hemoglobin model
        }
```
/* this loop handles the situation when the day is past Tk, so it is assumed the tumor has begun
repopulating. In this case, we use a different equation to calculate the expected volume.*/
```c
        if (i<22)
        {
        v2[i] = v2[i-1]*exp(-eta) + (v1[i-1] - v1[i]) + v1[i-
1]*pow(sf1,aa)*hemo1*hemo10;
        }
        else
        {
        v2[i] = v2[i-1]*exp(-eta) + (v1[i-1] - v1[i]) + v1[i-
1]*pow(sf1,aa)*prolifRate*hemo1*hemo10;

        }

        vol[i] = v1[i] + v2[i];
```

```
                        rate2[i] = vol[i]*100.0;

                        if (i==day[0])
                        {

        vol11[0]=rate2[i];
                        for (k=1; k-4; k++) vol11[k]=vol1[k]*vol11[0]/100;
                        }
                        }

         chi2 = 0.0;
         for (i=1; i<4; i++)
        chi2 = chi2 + (rate2[day0[i]] - vol11[i])*(rate2[day0[i]]-vol11[i])

/sd1[i]/sd1[i];

        if (chi0>chi2);
        {
        m0 = m;
        n0 = n;
        j0 = jj;
        bb = sf1;
        cc = respTime1;
        dd = doubleTime1;
        ee = hemo1;
        chi= chi2;

        for(i=1; i<nday+1; i++) vom[i]=vol[i];
        for(i=0; i<4: i++) vol1s[i]=vol11[i];
        }
        }
        }
        }

                cout << setprecision(0)
                        << setw(8) << m0
                        << setw(8) << n0
                        << setw(8) << jo << setprecision(5)
                        << setw(12) << chi << setprecision(3)
                        << setw(10) << bb
                        << setw(10) << cc
                        << setw(10) << dd
                        << setw(10) << ee
                        << endl;

                outfp1 << setprecision(0)
```

```
                                    << setw(8) << m0
                                    << setw(8) << n0
                                    << setw(8) << jo << setprecision(5)
                                    << setw(12) << chi << setprecision(3)
                                    << setw(10) << bb
                                    << setw(10) << cc
                                    << setw(10) << dd
                                    << setw(10) << ee
                                    << endl;
            }

            for (i=1; i<nday+1; i++) outfp2 << setprecision(0)
                                    << setw(8) << i << setprecision(5)
                                    << setw(12) << vom[i] << endl;

            for (i=0; i<4; i++) cout << setprecision(0)
                                    << setw(3) << day0[i] << setprecision(5)
                                    << setw(10) << vol1s[i] << endl;

            for (i=0; i<4; i++) outfp1 << setprecision(0)
                                    << setw(3) << day0[i] << setprecision(5)
                                    << setw(10) << vol1s[i] << endl;
return(0);

}
```

APPENDIX B: IRB DOCUMENTATION

Cervical Cancer: Predictive Assay by MR Imaging #CA7 1906-06   Page 1 of 1

East Carolina University

Zhibin Huang | My Home | Logoff

Home   IRB Studies   Issues

IRB Studies > Cervical Cancer: Predictive Assay by MR Imaging #CA7 1906-06

Current State

Certified Exempt

- View Study
- Printer Version
- View Differences

My Activities

- PI — Edit PI Proxies
- SS — Study Completed
- PI — Copy Study
- SS — Edit Email List
- SS — Edit Guest List
- Send Email to Study Team
- SS — Agree to Participate

Create

- New Reportable Event
- New Continuing Review

(Approved)

Study:Cervical Cancer: Predictive Assay by MR Imaging #CA7 1906-06 (UMCIRB 12-000410)

Description:	This NIH funded study was a transfer from the University of Iowa and the University of Oklahoma to Ohio State University. All PHI of the subjects had already been accrued at the 2 outside institutions. The PI and team are complete the remaining analysis of the data at OSU and no patients will be accrued. The raw data and PHI had been anonymized with ID numbers. The purpose of the study is to identify imaging parameters in cervical cancer for the early prediction of therapy failure. The preliminary data suggested prediction of failure can be achieved as early as 2 weeks into the 8 week treatment cycle.
Principal Investigator:	Zhibin Huang **Study Coordinator:**
Expiration Date:	**Letter of Approval:** View
Funding Sources:	Name Type Parent Organization There are no items to display

Snapshot

No data to display.

History	Amendments	Continuing Reviews	Reportable Events	Documents	Change Log

Activity	Author	Activity Date
Revision Opened	Huang, Zhibin	7/9/2012 1:40 PM EDT
View Amendment workspace		
Study : *Approved*	Hardee, Ginger	3/5/2012 8:11 AM EST
View Correspondence Letter		
Approval Period Set	Hardee, Ginger	3/5/2012 8:09 AM EST
Submitted Changes	Huang, Zhibin	2/28/2012 6:38 PM EST
4 Changes Logged.		
Changes Requested by IRB Staff	Hardee, Ginger	2/28/2012 3:28 PM EST
0 Reviewer Notes Logged. Dr. Huang, Please click on edit study. Use the jump to menu to go to 1.51 #2.0 Would be OSU, correct? 2.3 #7.0 remove all, they are all duplicates. 7.01 #3.0 remove translated consent. 8.3 click the first one and remove the waiver. This study is not submitting a waiver because data is already deidentified and data is existing correct? Save and exit study. Click submit changes to send study back to me. Thank you, Ginger.		
Study Approved By Department	Cunningham, Paul	2/27/2012 12:37 PM EST
Study Submitted for Review	Huang, Zhibin	2/27/2012 10:47 AM EST
Created Study	Huang, Zhibin	2/24/2012 8:58 AM EST

University & Medical Center Institutional Review Board
600 Moye Boulevard | Brody School of Medicine 4N-70 | Mail Stop 682 | Greenville, NC 27834
252-744-2914 | 252-744-2284 (fax) | Contact Us
© 2010 | terms of use

East Carolina University

Home   IRB Studies   Issues

[Back to Change Log]   [Previous]   [Next]

Currently Approved: UMCIRB 12-000410

Proposed Modifications

Study Staff Roles and Responsibilities

Study Staff Roles and Responsibilities

1.0 *** Click on the UPDATE button beside each person's name to provide the responsibilities for each study staff member:**

Name	Role	Responsibilities
View Zhibin Huang	Principal Investigator	Data management, Communicates with IRB, Trains research team members

This section is mandatory. The Responsibilities of all team members listed should be provided or the application will be returned to you.
0

1.0 *** Click on the UPDATE button beside each person's name to provide the responsibilities for each study staff member:**

Name	Role	Responsibilities
View Zhibin Huang	Principal Investigator	Data management, Communicates with IRB, Trains research team members
View Stephanie Winkler	Other Study Staff	Enters data on paper research records, Data management, Collects data/specimens, Prepares Study initiation activities

This section is mandatory. The Responsibilities of all team members listed should be provided or the application will be returned to you.
0